Improved prediction of iron losses using iGSEDC (iGSE under dc bias condition)

by

Asim Ali shah Syed

The University of Nottingham
PEMC Research group

Submitted to the Department of Electrical Engineering, Electronics
Computers and Systems
in partial fulfillment of the requirements for the Erasmus Mundus
Joint Master degree (EMJMD) in Sustainable Transportation and
Electrical Power Systems(STEPS)

at the

UNIVERSIDAD DE OVIEDO

September 2020

Author . . . .
Asim Ali shah Syed

Certified by. . . . .
Dr.Gaurang Vakil
Assistant Professor
Thesis Supervisor

Improved prediction of iron losses using iGSEDC (iGSE under dc bias condition)

by

Asim Ali shah Syed

Abstract

Design of most power conversion devices requires design of magnetic components and its prior knowledge of electrical performance. Core loss is vital information that design engineer requires during design stages of stator core of electrical machines.

In this thesis, iGSEDC method is proposed for predicting high frequency iron core losses under dc bias condition for non-sinusoidal excitations in electrical steels. In electrical machines, non-sinusoidal excitation waveforms have dc bias in minor loops unlike major loop. In this regard, single sheet magnetic sample of iron silicon alloy (10JNEX900) is utilized. Two experiments are performed. First experiment is performed using sinusoidal excitation under dc bias condition of 0 A/m, 10 A/m, 30 A/m & 50 A/m with frequency range of 100 Hz to 2 KHz. Results are curve fitted to yield four set of steinmetz parameters for each premagnitization (H_{dc}). Polynomial curve fit equations are obtained for each set of steinmetz parameters respectively as function of premagnitization (H_{dc}). It is also obtained from polynomial curve fit equation of dc B-H loop as function of dc bias (average flux densities of minor loops).Second experiment purpose is to measure specific losses for non-sinusoidal excitation waveforms of 100 Hz with different harmonic orders. These losses enable us to do sanity check compared to the results of iGSEDC, conventional iGSE and FTSE method.

It is found that iGSE under dc bias condition (iGSEDC) method estimate losses with error range of 1.55 % up to 6.2 %. On the other hand, conventional iGSE estimate losses with error range of 5.79 % to 16.12 %. Furthermore, both methods seem to perform in equal manner for non-sinusoidal excitation waveforms with no minor loops because there won't be any dc bias condition left. In addition to it, FTSE has variable trend and is most inaccurate method with errors in range of 2% to 41.6%.

Thesis Supervisor: Dr.Gaurang Vakil
Title: Assistant Professor

Acknowledgments

This dissertation is dedicated to

My beloved Parents (Baba saien and Ami jaan)

for their constant support ,encouragement and

unconditional love

Contents

List of Figures

List of Tables

Chapter 1

Introduction

1.1 Background

Efficiency improvements and reduction in losses are always desired when it comes to cost and durability of power electronic magnetic systems and electrical machines stator cores. Therefore global standards are in place to achieve targets of reducing losses. Motors and power electronic devices are largest users of energy therefore small improvements in losses will be considered significant and rewarding with respect to life cycle cost and improved performances. According to international energy agency, 40% of reduced green house emissions can be provided by energy efficiency alone. This led to increased transition of conventional vehicles into electric vehicles. According to electric vehicles initiative(EVI) which is a multi government policy forum enabling the awareness and adoption of electric vehicles worldwide. It is estimated that by 2030, market will have 30% more sales of electric vehicles. In addition to it, paris declaration on electromobility also stresses to have 100 million electric cars by 2030 that will encompass all type of road transport including pickup trucks and buses [9]. The main problem starts when design engineers starts to meet this increased demand because as per global standards,there is dire need to maintain energy efficiency with reduced losses and improved reliability. During transition to electric vehicles, researchers are aiming to go to the core of the reducing losses. Investigations starts with magnetic material with which magnetic components of power electronics systems and electrical

machines stator cores are developed. Researchers are investigating the way magnetic material is manufactured and losses are obtained for each manufacturing method. Manufacturing process affects the magnetic properties of material and its losses in general. Soft magnetic material found its potential applications in electrical machines development. Therefore, non grain oriented Fe-Si magnetic steel alloy is introduced for improved silicon content of 6.5% enabling low eddy current losses and high electrical resistivity in material. It is state of the art high frequency magnetic material for investigations for efficiency and losses improvements. There are dozen methods of iron loss estimation. Some methods require extra material characterization and physical parameters and some require only a steinmetz parameters.iGSE method is the most accurate Time domain method but it lacks dc bias condition. Therefore, new experiments under dc bias condition are done for improved iGSE method with dc bias condition for accurate core loss estimation in non-grain oriented magnetic steel material.

1.2 Importance of core Loss estimation under dc bias condition

Generally, time domain core loss estimation methods are accurate than frequency domain core loss estimation method where non-sinusoidal flux densities are involved. loss curves provided by manufacturer of soft magnetic materials does not include the losses that are caused by non-sinusoidal excitations. Furthermore, Loss curves found in data sheet of manufacturer are basically average loss data obtained as result of repeated measurements on similar material. It is for sinusoidal excitation waveforms and based on steinmetz equation. However, most electrical machines operate under non-sinusoidal excitation waveforms. Therefore, there is need of experimental loss data to be obtained under non-sinusoidal waveform excitation and estimated through analytical time domain method.

There is need of time-domain core loss estimation model to take into account the

losses under non-sinusoidal excitation waveforms encountered in stator core material of electrical machines. iGSE method is considered the most accurate method among family of steinmetz methods. However, it lacks dc bias condition that can be potential reason of its inaccuracies. In this regard, iGSE with dc bias condition method is developed where variation of steinmetz parameters corresponding to each dc bias flux density (average flux densities of major and minor loops) is considered .

1.3   Motivation and research Objective

An accurate time-domain core loss estimation model is needed for non-sinusoidal flux densities present in different parts of electrical machines. Losses are estimated well with respect to time varying field than in frequency domain because time varying flux density takes into account the 360° instantaneous values of flux density in calculation of losses. In addition to it, dc bias condition influence losses significantly. Therefore, iGSE with dc bias condition method is proposed. Research objectives are as under:

1. Determination of steinmetz parameters under dc bias condition for sinusoidal excitation. In this regard, measurement of losses are obtained for each range of frequencies (100 Hz, 300 Hz, 500 Hz, 700 Hz, 1100 Hz, 1500 Hz, 2000 Hz) against each flux density range (0.1 T,0.2 T,0.3 T,0.4 T,0.5 T,0.6 T,0.7 T,0.8 T,0.9 T,0.1 T) and results are curve fitted to obtain steinmetz parameters under dc bias condition of up to 50 A/m. On the other hand, another experiment is performed for obtaining total specific core loss (W/kg) due to each non-sinusoidal excitation waveform in single sheet magnetic material sample i.e. 10JNEX900. Five test signals are used with combination of harmonics. This study is done in chapter(3).

2. Steps for separation of major and minor loops are explained for non-sinusoidal excitation waveforms. Five test signals are used to investigate the separation of minor loops for higher harmonics. This study has been done in chapter(4).

3. iGSE with dc bias condition method is proposed with improved accuracies com-

pared to iGSE without dc bias condition. Absolute error percentage(%) for each signal is pictorially shown for iGSE with dc bias condition compared to conventional iGSE method and frequency domain method i.e. Fourier transform-steinmetz equation (FTSE). Results are presented in chapter(4).

4. Interior permanent magnet motor is designed. The flux densities are extracted from tooth of the stator and corresponding amplitude spectrum is obtained. This potential application for iGSE with dc bias method was proposed in chapter(5).

1.4   Tools used in research work

The main tool that was used is state of the art test bench with single sheet tester available in house. It is used to carry out AC/DC characterization for measurement of losses (w/kg) under sinusoidal excitation and non-sinusoidal excitation on single sheet magnetic sample. Core loss estimation is done using iGSE under dc bias condition method with separation of major and minor loops by developing scripts(file.m) using MATLAB. Furthermore, JMAG software is utilized (worked remotely on university desktop) for designing IPM motor.

Chapter 2

Literature review

In this chapter, section 2.1 includes state of the art advancement of high frequency non-grain oriented(NGO) silicon steel, and its importance in electrical machines' stator core for automotive. In addition to it, NGO electrical sheets grades of JFE Steel are discussed.Furthermore in section 2.2, determination of Iron losses in electrical machines are introduced and method to calculate total specific loss (W/kg) using single sheet magnetic material standard as per international standard IEC 6404-3 is presented and discussed.In addition to it, comprehensive review of iron loss models is done and then conclusion is inferred by comparing all iron loss models.

2.1 High frequency non-grain oriented silicon steel-Fe-Si

The need for magnetic materials has increased due to the transition of conventional vehicles into electric vehicles lately. High frequency and low loss magnetic material are of paramount importance for high speed passenger vehicles and specially for high power density machines of future electric pick up trucks. In addition to that, researchers are actively working towards increased efficiencies and reduced core losses in stator core of electrical machines to meet global energy efficiency goals as per paris climate agreements. Therefore state of the art high frequency non oriented Fe-Si

alloy (10JNEX900) is presented with magnetization and loss curves, obtained from data sheet of manufacturer. Steel materials are preferred choice for electrical machine designs of high speed automotive considering various factors. These include cost, sustainability with respect to high frequency, high power densities, specific losses(w/kg) and efficiencies.

Nowadays magnetic steel manufacturers design their materials with increased permeability and saturation levels with reduced specific iron losses. As market emerged with enlarged possible choices to design the machine with new magnetic materials, different compositions, and material processing techniques. The different forms of magnetic materials makes it a challenge for researchers and industrialist to choose the most suitable material for electrical machine design [10].

Most of the EV traction motors incorporate high frequency electrical steel as core material with high torque density and power density. Worldwide production of Fe-Si is around ten million tons annually and is the most common material for electrical machine applications. It has share of 80% of the total soft magnetic material market.On the other hand, the materials such as amorphous, powder,ferrite,Ni-Fe and cobalt-iron(Co-Fe) comprise of approximately 500 thousand tons only [11]. Having vast options and techniques associated with material choice for machine design have paved the way for choosing material on iterative basis. It is popular and important part of future machine development process. As rule of thumb, some material parameters are vital for machine design process i.e. magnetic saturation, coercivity, permeability, iron losses , magnetostriction, cost, delivery(forms, fully processed and semi-processed) and market availability [11].

Typical magnetic materials that are used in designing the electrical machines has the lamination thickness of 0.2mm to 1mm in case of iron typically the major component in the composition of material alloy. As matter of fact, Electric vehicles demand the need of reduced weight and optimal performances. Influence of magnetic materials on efficient design of electrical machines is well known.soft magnetic material with reduced weight and high performance are investigated. Soft magnetic materials are alloys with coercivity levels of up to 1000 A/m. For design process of high speed elec-

trical machines,it is important to understand the magnetic characteristics of magnetic materials that are usually obtained by testing the materials exposed to magnetic flux densities and range of frequencies but data available from manufacturers involves only magnetic characteristics corresponding to sinusoidal excitation measurements. It is stated in [12] that silicon iron alloys are widely used in electrical machines.

2.1.1 Importance of non-grain oriented silicon-iron steel alloy

Fe-Si alloy comes in two states i.e. grain oriented steel (anisotropic material and different permeability in different directions) and Non grain oriented steel (isotropic magnetic property in all directions).Grain oriented steels anisotropic properties are not utilized to date to its advantage,reluctance machine designs and new techniques to accommodate field weakening in high speed machines have potential application of GO steels [13].However Non-grain oriented silicon steel alloys are considered in automotive applications. Non grain oriented materials are used in rotational electrical machines because flux direction is usually not uni-directional in stator yoke of the rotational electrical machines. Iron content in Fe-Si alloys varies from 99 % in low Fe-Si steel alloys down to 93 % for highly alloyed Fe-Si steel.Whereas remaining content includes silicon(range 1 to 6.5%), aluminium (1 %), manganese (0.5 %). Silicon content enhances electrical resistivity but affects magnetic saturation. Similarly aluminium enhances electrical resistivity but affects the permeability of material.It is interesting to note that core losses manganese content have both positive and negative aspect as it yields higher permeability but also contributes to increased core losses.

2.1.2 Non grain oriented electrical Sheet (JNEX Core)

JNEX core is well balanced and feasible product of non-oriented electrical sheet produced by JFE Steel. It has high saturation magnetic flux density and low iron loss in the high frequency range. In general, electrical motors demand stator core with Fe-Si alloy with higher content of silicon i.e. 6.5 % as it has low eddy current losses.

It is also because of high speed,high torque and high power density requirements but it was thought to be impractical as material tends to be brittle and hard with addition of increased silicon content. Now manufacturers like JFE steels introduced their Fe-Si alloys(JNEX Core) eliminating this problem with their improved production processes namely through CVD process. JNEX-Core was successfully introduced with 6.5% silicon steel sheets to the world i.e. 10JNEX900 [2]. Furthermore, JFE Steel corporation is continuing to work towards meeting superior demands of future with advent of gradient high silicon Steel sheet [2]. DC characteristics of 10JNEX900 is shown in figure 2-1, Magnetization curves and usually known as B-H curve is shown in figure below where it clearly portrays its magnetic flux density and magnetic field saturation levels for the frequency range up to 50 KHz.
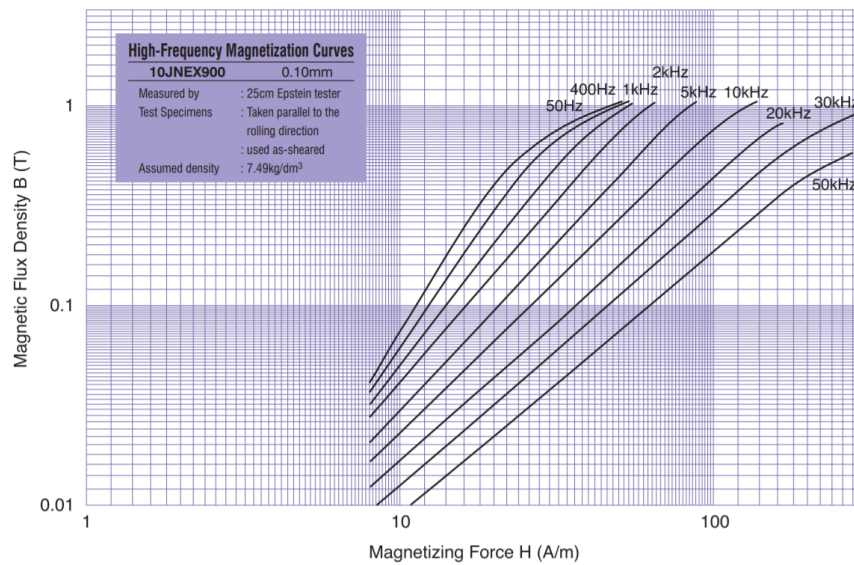
Figure 2-1: Magnetization Curves of 10JNEX900 [1]

In figure 2-2, AC characteristics of 10JNEX900 is shown. It includes High frequency core loss ranging from 50Hz to 50kHz. It is based on sinusoidal excitation based loss measurements. In figure shown below, the Core losses don't portray the behaviors of material in case of non sinusoidal magnetic flux densities. Hence there is a research potential lies for accurate estimation of iron stator losses with tests under non sinusoidal magnetic flux densities. That would be of great help in high frequency machine designs of the future.
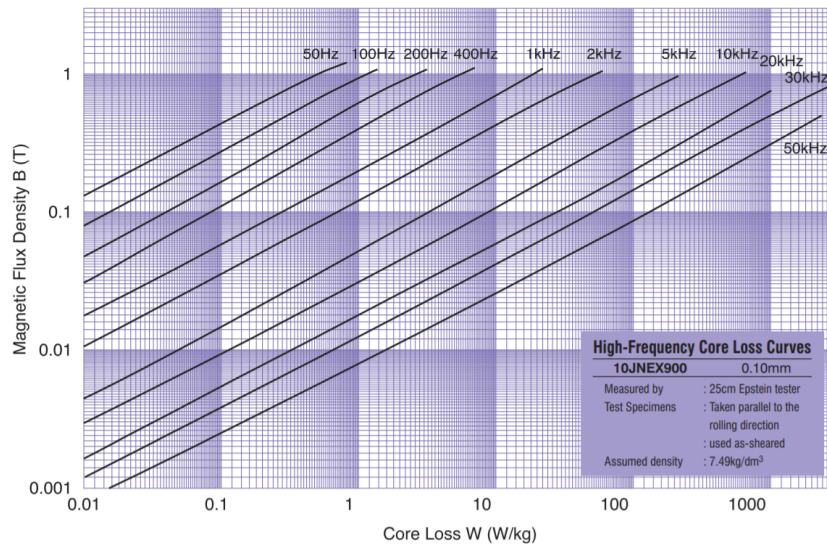
Figure 2-2: Core loss Curves of 10JNEX900[1]

DC hysteresis loops are shown for the flux density(B_m) range i.e.0.5T,0.7T,1T, 1.2T in figure 2-3 .
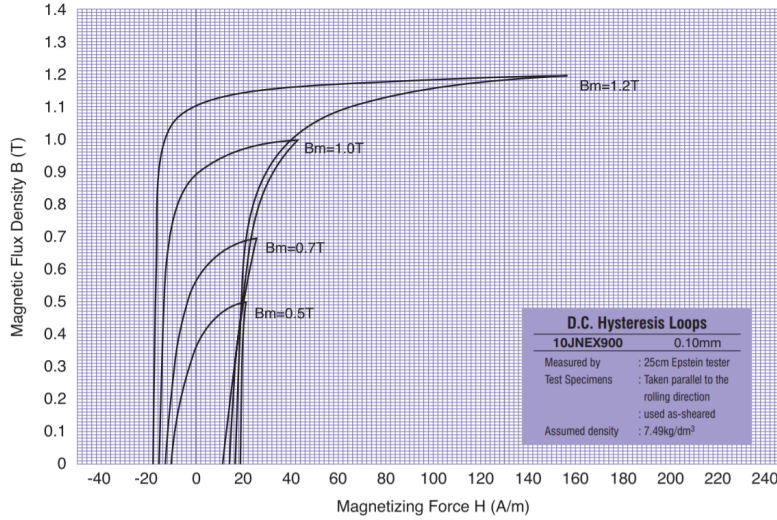
Figure 2-3: DC hysteresis loops of magnetic material i.e. 10JNEX900 [1]

10JNEX is grade of Super Core. Super Core grades find its applications in Automotive ,motors and in almost every power systems device. Its universal and robust nature can clearly be depicted from figure 2-4 .

Figure 2-4: Super core applications PI chart [2]

Super Core is best known available non-magnetic oriented Steel Sheets with superior performance [2]. One of the core design sample is shown as below in figure 2-5.

High frequency Core loss is greatly reduced due to high speed rotation using
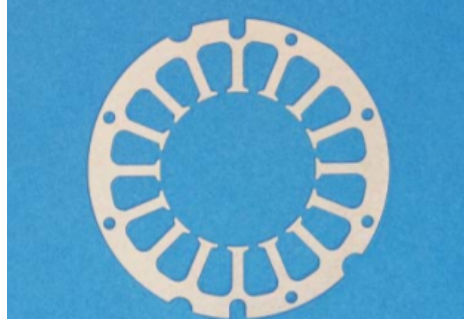
Figure 2-5: Example sample for core design [2]

laminated core in motors and cores are produced using stamping lamination process making it viable for high frequency applications unlike conventional steel material with 3% silicon content [2] . Example laminated core design is shown in figure 2-6.
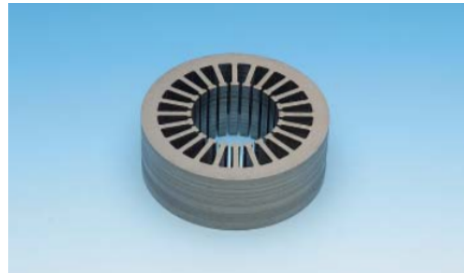
Figure 2-6: Example of laminated cores for motor [2]

2.2 Determination of iron losses in electrical machines

Iron losses play important role in the optimization and design process of electrical machines.Generally losses are reduced in the machines by using low loss Fe-Si steel alloy and new composite materials [3].There is dire need of improved efficiencies and reduce energy consumption of electrical machines as per European commission regulation (EC) NO 640/2009. There are several factors that can contribute to the losses in the machines i.e. electromagnetic iron losses. It is usually occur in stator teeth, stator yoke and rotor yoke. Iron losses are significant during field weakening operation of electrical machine.Usually Electrical machines conduction losses in ferromagnetic

materials are ignored as these occurs in MHz range only. However Hysteresis losses and Eddy current losses are considered to be occurring due to same phenomenon i.e. every change in magnetization causes moments in domain walls and create in turn eddy currents and consequently joule heating. However hysteresis losses also considered to be occurring at zero frequencies because even if magnetization change is very slow, magnetization inside the domain locally change very rapidly and discrete in time causing eddy current losses [3].

2.2.1 Magnetic measurement Standard based single sheet tester(SST)

Iron losses were discovered for almost more than 100 years ago but there is still some discrepancy between measurement results and loss prediction results. One of the challenge is as there is no physical way to measure losses in the magnetic materials directly. IEC and ASTM standards determine losses by preparing special shaped lamination magnetic material sample with an Epstein frame or by ring specimen measurements using ring shape probes [8]. These measurements are based on electrical winding which create magnetic fields in the laminated sample under investigation while magnetic flux density in the material is obtained from secondary winding, where induced voltage is caused by changing magnetic fields in magnetic sample. That's where iron losses are found using magnetic field (H) and the flux density (B) inside the material. Furthermore, iron loss measurements can be utilized as material input parameters for calculating iron losses in electrical machines using FEM simulators.

The method is applied and investigations are done for accurate core loss estimation in single rectangular sheet sample of magnetic material i.e. 10JNEX900. Experimental analysis is described in detail in chapter 03 as per EN IEC 6404-3 standard. This standard is the 3rd edition prepared by iron and steel and non ferrous metals committee and its overview is sourced from [14]. This method scope includes determination of excitation current, measurement of magnetic field strength and specific apparent power.

2.2.2 Measurement of total specific loss

Single sheet tester is applicable for test specimen which are obtained from magnetic sheets. General principle of this method is based on a sample of magnetic sheet and placed between two windings i.e. primary (exterior/ magnetizing) and secondary(interior/ voltage) winding. Power supply should be of low internal impedance and highly stable in terms of voltage and frequency.During measurement,it is recommended that voltage and frequency is kept constant within percentage error of 0.2%. In addition to it, induced voltage in secondary should be kept sinusoidal within maintained form factor of 1.111 with percentage error allowance of 1%. It is done by using many means, one way is to use electronic feedback amplifier. total loss measured by the circuit is shown in figure 2-7 below:
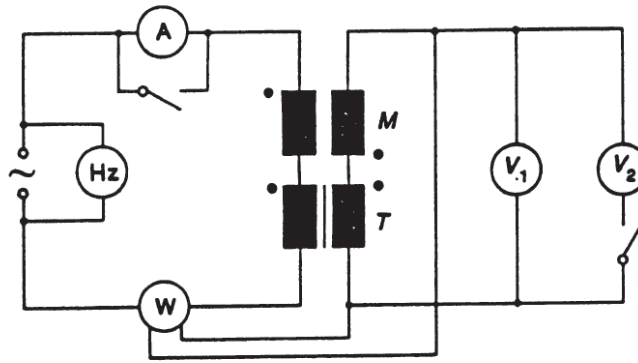
Figure 2-7: circuit for determination of total specific loss
[14]

Power measurement is made by wattmeter having accuracy of 0.5% or better at actual power factor and crest factor. Secondary rectified voltage is measured using average type voltage meter V1. In addition to it RMS volt meter V2 is also used. Mutual inductor M is placed with test frame T(primary winding to secondary winding connection) for air-flux compensation.

Source is adjusted to average value of secondary rectified voltage. its expression is shown in equation (2.1).

$$\overline{|U_2|} = 4fN_2\frac{R_i}{R_i + R_t}A\hat{J} \tag{2.1}$$

23

where

$\overline{|U_2|}$ is the average value of secondary rectified voltage ;

f is frequency in,Hertz ;

R_i is the combined resistance of all secondary instruments in ohms;

R_t is the series resistance of secondary windings in ohms ;

N_2 is the number of turns of secondary winding ;

A is the cross sectional area of test specimen ;

$\hat{J}$ is peak value of magnetic polarization,in tesla ;

Cross sectional area A is obtained by following relation:

$$A = \frac{m}{l\rho_m} \tag{2.2}$$

where

m is the mass of specimen, in kilograms;

l is the length of test specimen, in meters ;

ρ_m is the density of test material, in kilograms per cubic meter ;

Total specific power loss is obtained by using equation (2.3).

$$P_s = \left[P\frac{N1}{N2} - \frac{(1.111(\overline{|U_2|})^2)}{R_i} \right] \times \frac{l}{ml_m} \tag{2.3}$$

Where

$\overline{|U_2|}$ is average value of secondary rectified voltage,in volts;

P_s is the specific total power loss of the test specimen, in watt per kilogram;

P is the power measured,in watts;

m is the mass of the test specimen,in kilograms ;

l_m is the conventional magnetic path length in metres $l_m = 0.45m$

l is the length of test specimen,in meters ;

N1 is the number of turns in primary winding

N2 is the number of turns in secondary winding ;

R_i is the combined resistance of instruments in secondary circuit,in ohms ;

2.3 Steinmetz based iron loss models

C.P steinmetz is known to be pioneer of core loss estimation due to his contribution in [15] for calculation of losses in magnetic materials in 1892 and he presented his work in American institute of engineers (AIEE). He coined the empirical formula for calculation of losses in equation 2.4

$$P_v = \eta \times B^{1.6} \tag{2.4}$$

where

P_v is losses during whole magnetization cycle ;

η is material constant ;

B is Peak value of magnetic flux density ;

Generally core loss estimation is based on power law equation that is named after steinmetz due to his historic work in [15] for calculation of re-magnetization losses using an empirical equation that does not have any frequency dependence as shown in 2.4. However the equation 2.5 is used and named after C.P steinmetz [4].

$$\overline{P_v(t)} = k \times f^\alpha \times B^\beta \tag{2.5}$$

where

P_v is time average power loss per unit volume ;

k,α, β are the material constants known as steinmetz parameters ;

f is frequency of magnetization in Hertz for sinusoidal excitation ;

B is Peak value of flux density waveform ;

Design of Electrical machines and its optimization require prediction of losses. Engineers and researchers select the methods suitable to their application as per available parameters, availablity of testing facility and accuracy requirements. steinmetz equation and data provided by manufacturers of magnetic materials are valid for sinusoidal excitation only. On the other hand, in modern applications such as in-

creasing electrical machines and switching power converters have non-sinusoidal wave forms. In additon to it, dc bias also affects losses [4]. Therefore, there is need of investigation for accurate core loss estimation model that can be valid for non-sinusoidal excitation wave forms. In addition to it, steinmetz parameters need to be determined through curve fitting techniques for sinusoidal excitation waveforms under dc bias condition.

Overview of various iron loss models is depicted in 2-8. some of them are discussed in detail with an additional FEMM based advance core Loss model with state of the art formulas by JMAG (a machine design software) are discussed. In the end, conclusion is inferred for the suitability of the method followed in our experiments over other methods.
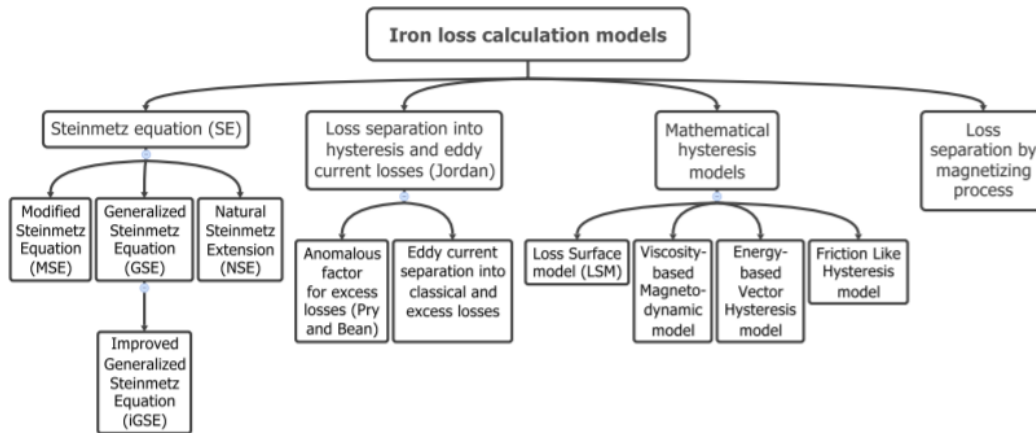
Figure 2-8: Approaches for estimation of iron losses in Electrical machines[3]

2.3.1   Modified steinmetz equation-MSE

The first time domain steinmetz based core loss estimation model is Modified steinmetz equation. It is introduced when authors in [16] felt the need of core loss estimation model for non-sinusoidal wave form excitation. Motivation was taken with the concept of macroscopic re-magnetization rate i.e. dM/dt is in direct relation with core losses. Therefore frequency of steinmetz equation was replaced with physical loss

parameter dM/dt that is directly proportional to magnetization rate dB/dt. Firstly induction rate is averaged over complete re-magnetization cycle from maximum induction sample to minimum induction sample and vice versa in equation 2.6 below.

$$B' = \frac{1}{\Delta B} \times \oint \frac{dB}{dt} dB \qquad \Delta B = B_{max} - B_{min} \qquad (2.6)$$

Furthermore,equation 2.6 can be represented as transformed form in equation 2.7

$$B' = \frac{1}{\Delta B} \times \int_0^T \left(\frac{dB}{dt}\right)^2 dt \qquad (2.7)$$

Finally relationship is established between re-magnetization frequency (f) and averaged re-magnetization rate (B') in 2.8, where equivalent frequency f_{eq} is calculated considering the normalizing constant $\Delta B^2 * \pi^2$.

$$f_{eq} = \frac{2}{\Delta B^2 \pi^2} \int_0^T \left(\frac{dB}{dt}\right)^2, dt, \qquad (2.8)$$

Originally power loss per unit volume "$P_v = Kf^\alpha B^\beta$" need to be adapted for calculation of energy dissipated e_d in complete cycle of magnetization therefore period is multiplied on both hand sides to get expression of modified steinmetz equation incorporating equivalent frequency,simplifying the relation as under in eq:2.9

$$e_d = \frac{P_v}{f} = \frac{Kf^\alpha B^\beta}{f} \qquad (2.9)$$

Therefore specific energy loss becomes power gain "P_{loss}" because every re-magnetization cycle is determined from the equivalent frequency relation in 2.8. This specific energy loss formula in 2.10 is similar to steinmetz equation that is used to calculate losses for non-sinusoidal magnetic flux density waveforms.

$$e_{loss} = k \times f_{eq}^{\alpha-1} \times \widehat{B}^\beta, \quad where \ \widehat{B} = \frac{\Delta B}{2} \qquad (2.10)$$

When there is repetition of re-magnetization with period $T_r=1/f_r$ the power losses relation can be expressed as in 2.11.

$$P_{loss} = \left(k \times f_{eq}^{\alpha-1} \times \widehat{B}^{\beta} \right) * f_r \tag{2.11}$$

This method was meant to calculate iron losses for arbitrary flux density waveforms. The draw back of this method was that the calculated losses was too small and inaccuracies was recorded for increasing harmonics' amplitudes. Furthermore losses turned out to be discontinuous function of continuous change of parameters [4].

2.3.2 Generalized steinmetz equation-GSE

In 2001,new method was proposed in [17] to overcome the inconsistency of steinmetz equation 2.5 with MSE approach in calculation of losses. This new method was based on the concept of instantaneous core loss. It was based on Hypothesis that instantaneous core loss is based on two essential points unlike MSE approach as follows :

1. instantaneous flux density B(t).

2. instantaneous flux changing rate dB/dt.

Single valued function depicting B(t) and dB/dt is shown in equation 2.12

$$P_v(t) = P_d\left(\frac{dB}{dt}, B\right) \tag{2.12}$$

instantaneous losses can be calculated Using GSE shown in equation 2.13

$$P_v(t) = k_1 \times \left|\frac{dB}{dt}\right|^{\alpha} \times |B(t)|^{\beta-\alpha} \tag{2.13}$$

To be consistent with steinmetz equation, parameter k_1 should be defined as in equation 2.14

$$k_1 = \frac{k}{(2\pi)^{\alpha-1} \int_0^{2\pi} |cos\theta|^{\alpha} |sin\theta|^{\beta-1} d\theta} \tag{2.14}$$

28

Therefore mean value over the time period 'T' will be expressed as shown in equation 2.15.

$$P_v(t) = \frac{1}{T} \times \int_0^T k_1 \times \left|\frac{dB}{dt}\right|^\alpha \times |B(t)|^{\beta-\alpha} dt \qquad (2.15)$$

The drawback of this method is when it shows significant inaccuracies when it shows deviation with regard to experimental data exactly at the point where minor hysteresis loops starts appearing in flux density waveform [4]. Its limitation comes with waveforms containing high number of harmonics. In addition to it, this form of equation is not valid when $\alpha > \beta$ because iron losses would go infinite [18]. Furthermore,since losses only depend upon instantaneous values of flux density ignoring the time history of flux density waveform causing another reason for inaccuracies in calculation of losses [4]. These shortcomings are met by improved version of GSE i.e. improved general steinmetz equation in [4].

2.3.3 Improved generalized steinmetz equation-iGSE

This method was proposed in 2002 in [4] improving the concepts and ideas of general steinmetz equation. Instantaneous core loss is calculated using amplitude of major and minor loops where flux density is instantaneous. Therefore instead of using B(t), it utilizes ΔB yielding final expression for time average loss is follows as in equation 2.16.

$$P_v(t) = \frac{1}{T} \times \int_0^T k_1 \times \left|\frac{dB}{dt}\right|^\alpha \times |\Delta B|^{\beta-\alpha} dt \qquad (2.16)$$

where ki is obtained by steinmetz parameters in following expression in equation 2.17.

$$k_1 = \frac{k}{(2\pi)^{\alpha-1} \int_0^{2\pi} |cos\theta|^\alpha |2|^{\beta-\alpha} d\theta} \qquad (2.17)$$

Higher accuracies of this method are endorsed in [19] and [20]. This method and formulation calculate losses appropriately in presence of minor loops [4]. Algorithm to separate minor and major loops are shown in section 2.3.3.

Algorithm for extraction of minor loops

it is essential for separation of minor loops that algorithm should be able to extract minor loops up to any number of nested levels in any arbitrary non-sinusoidal waveform. Authors proposed a method shown in [4] those steps can be summarized as below:

1. Successive values of flux density is stored in major loop until minor loop is detected using change in slope from positive to negative

2. When minor loop starts, elements of it are stored in a new vector array as collection of minor loop as first minor loop vector. it stores minor loop elements until flux density values rises back to same value where it started decreasing or where it marks the closure of minor loop.

3. After the minor loop closes,major loop continue to store the collection of flux density values.

4. If minor loop is detected again , it will be stored in a same minor loop vector. Minor loop vector stores all collection of minor loops.

5. similarly any sub-loops within minor loops will also be extracted.

6. Finally loss calculation is done using equation 2.16 for respective major and minor loops and then total loss is found by weighted average, taking into account the contribution of each minor loop by using the fraction of total period each loop occupies. The expression is as under in equation 2.18

$$P_tot = \sum_{n=\iota} P_\iota \frac{T_\iota}{T} \tag{2.18}$$

The algorithm with steps followed in separation of minor loops is depicted in figure 2-9

This method is good and known to be accurate for only some conditions. However it don't take into account the dc bias effects that is the possible reason of inaccuracies
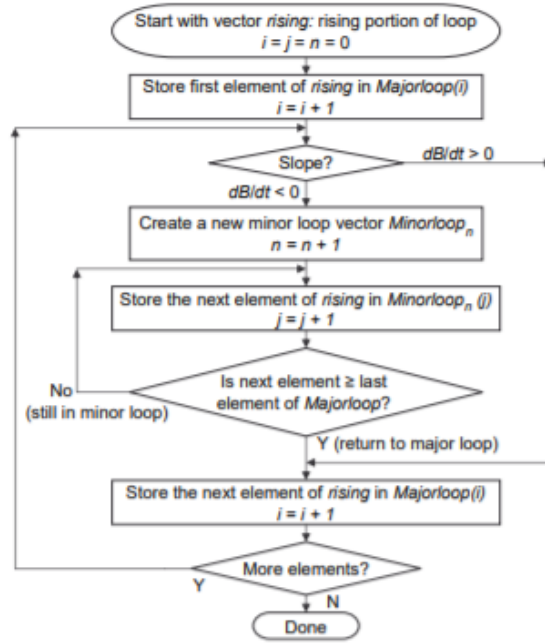
Figure 2-9: Steps for Separation of minor loops [4]

in loss calculations for most of the waveforms. The iGSE approach is also sensitive to values of Steinmetz parameters, mainly α and β tend to vary for waveforms having harmonic content over wide range of frequencies.In addition to it, this method also don't consider the magnetic relaxation effect that further work has been done by authors in [21] in calculation of losses. Furthermore, this method is named as i^2GSE discussed in section: 2.3.5. However, there is good potential of further investigations to be done for curve fitting to get Steinmetz parameters for sinusoidal experimental data of high frequencies and propose variation of Steinmetz parameters due to dc bias effects to prevent inaccuracies in calculation of losses.

2.3.4 Natural Steinmetz extension-NSE

This approach is similar to IGSE and proposed by authors in [22]. Using Natural Steinmetz equation- NSE, losses can be calculated averaged over one period is as

under in equation 2.19;

$$P_v = \frac{\Delta B^{\beta-\alpha}}{2} \frac{K_N}{T} \int_0^T \left| \frac{dB}{dt} \right|^\alpha dt \qquad (2.19)$$

The parameter K_N, a constant that is determined by using equation 2.20 shown below
;

$$k_N = \frac{k}{2\pi^{\alpha-1}} \int_0^{2\pi} |cos\theta|^\alpha d\theta \qquad (2.20)$$

This approach of natural steinmetz extension (NSE) was primarily proposed for power electronics applications where square waves are used based on duty ratios. In this approach, authors of [22] compared NSE with MSE having SE as baseline and tested for large variation of duty ratios. Results of NSE matched with the experimental data for commercial ferrite grades. Both MSE and NSE tend to give same numerical results at duty ratio D=0.5 with α =1 (pure hysteresis losses) or α= 2 (Foucault losses) [22].

2.3.5   Improved-improved generalized steinmetz equation-i^2GSE

Improved-Improved generalized steinmetz equation is the extension of iGSE approach taking into account the relaxation effects to the core loss[21]. Due to this, magnetization will change even if field is constant or magnetization gets delayed. However, iGSE gives zero core losses when magnetic flux density is constant since dB/dt will tend to become zero but losses still occur and that would be because of relaxation processes in magnetic materials. In short, relaxation process depend upon residual losses, such relaxation processes becomes important in high frequency and pulsed field application and when thermal equilibrium of magnetic system changes enabling system to move rapidly towards new equilibrium state (thermal). In addition to it, shape of B-H loop changes with respect to rate of change of applied field(rate-dependent loop) [21]. The time average specific core loss density is calculated as under in equation 2.21.

$$P_v(t) = \frac{1}{T} \times \int_0^T k_1 \times \left|\frac{dB}{dt}\right|^\alpha \times |\Delta B|^{\beta-\alpha} dt + \sum_{l=1}^{n} Q_{rl} \times P_{rl} \qquad (2.21)$$

The time average core loss(P_{rl}) due to l_{th} of n transients to zero voltage.It is calculated as under in 2.22

$$P_v(t) = \frac{1}{T} \times k_r \times \left|\frac{dB(t-)}{dt}\right|_r^\alpha \times |\Delta B|^{\beta_r} \times \left(1 - e^{\frac{-t1}{\tau}}\right) \qquad (2.22)$$

where,

P_{rl}= losses due to relaxation process ;

$\frac{dB(t-)}{dt}$= the flux density before switching ;

τ =time constant for relaxation process ;

n = number of phases with constant flux ;

t_1= duration of phase during constant flux ;

The relaxation processes are defined using exponent 'e' so that losses don't increase when $t_1 > 5\tau$ is valid. Relaxation processes consideration can be avoided for low frequencies .

Limitation of this method is the need of additional measurements for material constants(different from normal steinmetz parameters) i.e. α_r, β_r, k_r and τ. i^2GSE is used in Power electronics applications [21].

2.3.6   Fourier transform steinmetz Equation-FTSE

In literature , FTSE is not an valid approach for calculation of losses as its non linear phenomenon [19]. Yet many people prefer to use it mostly in industries compared to iGSE method because of complexities involved in iGSE and calculation of its material constants variation with dc bias. In [19] authors tried to shed the light on FTSE accuracies including the benefits of iGSE.

For finding the core loss using Fourier transform steinmetz equation method, flux density is decomposed into its harmonic components firstly then steinmetz equation is applied to each component say i.e. i up to n then added losses of each component

using equation 2.23 for i_{th} of n cycles for each experimental variation. Hence it is calculated using following relation ;

$$P_v(t) = \frac{1}{n} \times \sum_{i=1}^{n} K_i \times f_i^{\alpha} \times B_i^{\beta} \tag{2.23}$$

It is concluded in [19] that FTSE is used in industries for calculation of losses in non-sinusoidally excited transformer cores. It is also stressed that it is relatively accurate for 10% THD sinusoids and triangular excited cores for low flux densities but inaccuracies were claimed for square waves tests performed. However their claim is based on core material of epcos N87 ferrite core and further investigations are needed for its validity on wide scale range of frequencies and newer magnetic material grades.

2.3.7 Core loss model based on steinmetz premagnitization graph(SPG)

In this method, dependency of α, β and k is shown on premagnitization H_{dc}. Extensive measurements were performed on ferrite material for frequencies up to 100 KHz for power electronics application for triangular current/flux shape. Therefore new equation was derived for this particular application as under:

$$P_v = ki(2f)^{\alpha} \Delta B^{\beta} \tag{2.24}$$

Where parameters are similar to the parameters defined for iGSE relation in equation 2.16.

In this method, authors in [23] confirmed that alpha is independent of dc bias condition by observing the straight line slopes in the logarithmic plot of frequency vs total power losses for frequencies up to 100KHz. In the same way ΔB was varied in x-axis logarithmic scale against power losses in y-axis and it was found that losses don't follow straight line anymore. In addition to it, k also don't follow straight line when losses in y-axis were plotted against premagnitization H_{dc}. Hence it was

concluded that steinmetz parameters except α are dependent on dc bias condition and there is need of variation of beta and k parameters except alpha in calculation of total specific power losses. Also accuracy of this method is justified for flux densities up to 200 mT.

There is need of explanation for core loss estimation using time domain iGSE for Non-sinusoidal waveforms with various harmonics with increased flux densities up to 1.2T to get accurate core loss estimation for novel machine designs of motors. Furthermore time domain equation i.e iGSE need to be investigated and explained for measurement of losses in novel magnetic materials with 6.5% silicon content and explained. This study is carried out in chapter (4).

2.4   Loss surface model

This losses surface model was first introduced in 2000 by authors in [24]. It is scalar and dynamic hysteresis model named as loss surface model. In this approach, surface function S is used to determine the magnetic field H.The relation is shown in eq:2.25

$$S = H\left(B, \frac{dB}{dt}\right) = H_{stat}\left(B\right) + H_{dyn}\left(B, \frac{dB}{dt}\right), \qquad (2.25)$$

loss surface function S is separated into two parts i.e. static and dynamic part. This model links magnetic field H on sheet surface while flux density B in the thickness of the sheet.The static part is usually modelled by Preisach model which is rate-dependent.Input values are determined by measuring values of major loops and first order reverse curves. On the other hand dynamic part is dependent on two linear analytical equations which describe the low and high values of magnetic flux density derivative i.e. dB/dt after subtracting the magnetic field intensity H_{stat} [8].

Further improved loss surface model is proposed by author in [25] on loss surface model where they are considering instantaneous power loss computation instead of average loss for entire cycle of flux density waveform. relation in equation 2.26 is used. This new approach assumed that if magnetic flux density B and dB/dt are

known then material behaviour can be well anticipated. The surface in a B-dB/dt is taken from measurements. Measurements are done as per IEC standard 60404-4 and corresponding methods in [14]. In this approach, triangular waveform is optimum choice because of the reason of its constant $|dB/dt|$

$$p_v \left(B(t), \frac{dB(t)}{dt} \right) = P_v \left(-B(t), \frac{-dB(t)}{dt} \right) \tag{2.26}$$

This approach enables user to avoid extra measurements required for additional parameters and this method considers the degradation of material due to cutting processes as well. However extensive experiments and modelling effort involved in this method comes as one of its negative points after all benefits. However it is known to give good performance.

2.5 Loss separation approach

In [26], jordan separated the losses into two components i.e. hysteresis and eddy current loss components. It is shown in equation 2.27.

$$p_v = \rho_h + \rho_e = k_h \times \hat{B}^2 + k_e \times (f \times \hat{B})^2 \tag{2.27}$$

where
ρ_k —-hysteresis losses ;
ρ_e —-the eddy current losses ;
k_e and k_e —material constants ;

This approach of H.jordan known to be inaccurate and obsolete for novel materials. However this work helped to a great extent to researchers. Bertoti in [27] extended the loss separation formula with addition of excess loss term. Bertotti explained the difference between experiments and predicted results were taken into account as in equation 2.28

$$p_v = \rho_h + \rho_e = k_h f \hat{B}^2 + k_e (f\hat{B})^2 + k_{ex}(f\hat{B})^{\frac{3}{2}} \tag{2.28}$$

If equation 2.28 is divided by frequency then it will be valid for single losses occurring for one period of flux density B with frequency f. The relation for single losses or energy losses is indicated in equation 2.29. [28]

$$\frac{p_v}{f} = w_h + w_e = k_h \hat{B}^2 + k_e f (\hat{B})^2 + k_{ex} f^{\frac{1}{2}} (\hat{B})^{\frac{3}{2}} \tag{2.29}$$

With increasing frequencies , hysteresis losses stay constant while eddy current and excess losses increases. This method is considered when power devices are exposed to flux densities with high harmonic contents where it is not sinusoidal anymore.

Hence it is evident from literature in [8] that equation 2.28 is known to be accurate for nickel iron alloys but not for silicon iron alloys. Therefore several correction factors were introduced and the loss separation equation 2.28 is improved by introducing some changes from time to time. It is later then realized from literature study in [8] that hysteresis losses of silicon iron alloys (laminated sheets) don't fit the squared flux density dependency then α the fitting co-efficient was introduced then equation becomes the equation 2.30

$$p_v = k_h + k_e = k_h f \hat{B}^\alpha + k_e f^2 (\hat{B})^2 + k_{ex} f^{1.5} (\hat{B})^{1.5} \tag{2.30}$$

where

Excess loss factor—- $K_{ex} = \sqrt{SV_o \sigma G}$;

Eddy current loss factor—-k_e is approximated from max-well equation in 2.31 ;

$$k_e = \frac{d^2 * (dB(t)/dt)^2}{12 * \rho * \gamma} \tag{2.31}$$

Hysteresis loss factor i.e. k_{hys} is proportional to hysteresis loop area of the material at low frequencies. However this method requires additional parameters knowledge involved in excess loss correction factor which needs corresponding physical parameters i.e. cross sectional area of laminated sample, co-efficient of eddy current damping , σ lamination sheets' electrical conductivity where as V_0 takes into account the grain size after characterizing statistical distribution of coercive fields.Furthermore the specific

resistivity ρ and γ, material density of lamination sheets are needed for calculation of eddy loss co-efficient k_e [8].

2.6 Physical based models

Physical models are used to describe material behaviour. However these models use more material parameters and increased computation times are needed because of higher accuracies involved. Hysteresis loop is described in a mathematical way just as in empirical method. As it tries to reproduce the hysteresis behaviour [5]. The relation that is used to calculate losses arising from change of magnetization is calculated with BH integral as indicated in equation 2.32

$$e_v = \int H dB \tag{2.32}$$

Equation 2.32 shows the enclosed area of hysteresis loop and has the dimension of energy per volume. By multiplying equation 2.32 with the frequency of magnetization, we get relation for calculation of losses in equation 2.33

$$e_v = f_r \int H dB \tag{2.33}$$

2.6.1 Preisach model

This model was introduced in 1935 by F.Preisach [29] and comprehensively discussed in [5]. Its principle is based on weighted superposition of many so called Preisach hysterons (HR). The relationship of in and output of the hysteron is depicted in figure 2-10

It is shown in figure 2-10 that output can be between -1 and 1. When upper switching threshold α is exceeded from a level below α then output will drive to high state. When input falls below the lower switching threshold β then output will drive into low state. However if input is in between the two threshold switching levels then output will retain its previous state. Magnetic material behaviour is described by

38
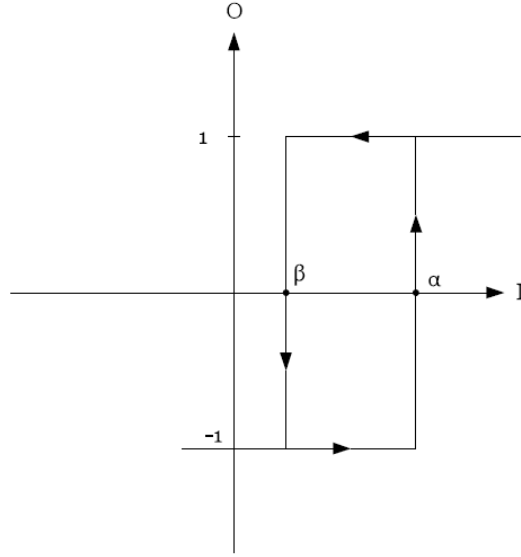
Figure 2-10: Hysteron with Switching thresholds of α and β [5]

parallel connection of many hysterons and weighting their respective outputs. It is shown in figure 2-11 below ; Each hysteron will have its own switching thresholds. The Presach function calculated the weighting factors i.e. $u_x(\alpha_x, \beta_x)$. Loss behaviour can be described by increasing the number of hysterons and when n becomes infinity then discrete hysteresis loop turns to be continuous one. Hence output of the whole system can be found by as in equation 2.34

$$O(t) = \int \int_{\alpha >= \beta} \mu(\alpha, \beta) O_{\alpha, \beta}(t_0, n_0) I(t) d\alpha d\beta \qquad (2.34)$$

In magnetic systems considered in this case, input is magnetic field and output is magnetization of the material. The model considered here describes the static hysteresis and rate of change is neglected. Dependency of weighting function is dependent on rate of change of output $\frac{dO(t)}{dt}$ so equation 2.34 becomes :

$$O(t) = \int \int_{\alpha >= \beta} \mu\left(\alpha, \beta, \frac{dO(t)}{dt}\right) O_{\alpha, \beta}(t_o, n_o) I(t) d\alpha d\beta \qquad (2.35)$$

39
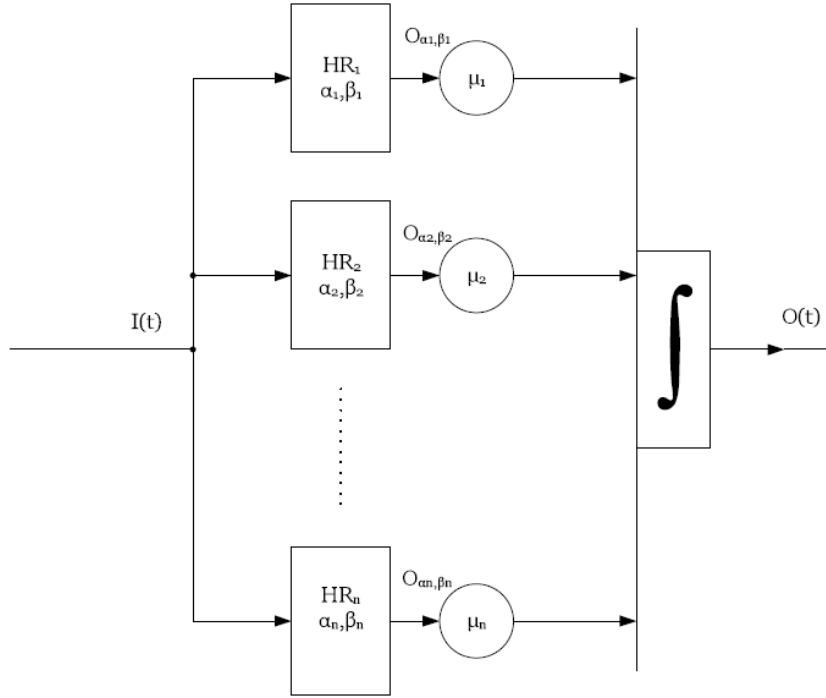
Figure 2-11: Single hysterons' parallel connection [5].

2.6.2 Jiles Atherton Model

This approach is based on the method presented by jiles in [30], magnetic material behaviour is expressed using differential equation having used the Langevin function as shown below in equation 2.36

$$L(x) = coth(x) - 1/x \qquad (2.36)$$

Initial magnetization curve is used when magnetic material shows no hysteresis behaviour. This waveform is approximated with langevin function. Calculation of magnetization is done using following differential equations in 2.37 and 2.38 [31].

$$M_{an} = M_s \left[coth\left(\frac{H + \alpha M}{a} \right) - \frac{a}{H + \alpha M} \right] \qquad (2.37)$$

$$\frac{dM}{dH} = (1-c)\frac{M_{an} - M}{k\delta - \alpha(M_{an} - M)} + c\frac{dM_{an}}{dH} \qquad (2.38)$$

where,

M_{an} .... anhysteretic magnetization ;

M_s .... saturation magnetization ;

$a,\alpha,c,$k ..... material parameters ;

The material parameters a and α has an influence on shape of hysteresis loop, whereas k and c affect the width and M_s the height respectively.δ is the sign$(\frac{dH}{dt})$ function which distinguishes between ascending branch i.e. $\left(\text{sign}(\frac{dH}{dt}) = 1\right)$ and the descending branch $\left(\text{sign}(\frac{dH}{dt}) = \text{-}1\right)$ [32]. Jiles atherton model becomes inaccurate when asymmetrical excitations or distorted hystersis loops are involved as discussed in [5]. However in [31] improved jiles atherton model showing dependence of parameters are shown and distorted hysteresis loops are taken into account and behaviours related with increasing frequencies are considered too in improved jiles atherton model. This approach is expressing the single parameters as function of the magnetic field. Parameters and magnetic field relationship can be linear one and specifically as in [31] combination of excitation dependent factor and constant. The only draw back in [31] that it needs increased number of parameters determination but it delivers accurate results.

2.7   Advance iron core loss model

There are two methods that can be used to calculate iron losses and iron loss density generated in magnetic materials in FEMM based software i.e. JMAG. Iron losses calculated by following solvers

1. Magnetic field analysis solver :

2. Iron losses analysis solver :

2.7.1 Iron loss calculation using magnetic field analysis solver

It considers iron loss effect during magnetic field analysis but without iron loss condition.Iron loss is calculated as sum of hysteresis and joule loss. Similarly iron loss density can be determined. In addition to that,Hysteresis loss and joule loss are calculated during each step in magnetic field analysis.It requires time to converge but has good precision results close to physical phenomena. Analysis flow chart Using FEMM tool i.e. JMAG is described brefly as under:

1. Magnetic field analysis study is created that can be static analysis,transient response analysis and frequency response analysis. It can be implemented in FEMM model of any dimension i.e. 3-dimensional, 2-dimensional or axissymmetric.

2. Parameters are set that are necessary for calculation of iron losses. Required setting are set for both hysteresis loss and joule loss (eddy current loss) calculation as per set procedure in [6].

3. Magnetic field analysis study is finally executed. It can be done using JMAG designer, JMAG scheduler or command line.

2.7.2 Iron loss calculation using iron loss solver

Iron loss analysis is done with magnetic flux density distribution data obtained from magnetic field analysis with iron loss condition. It requires short computation time due to post processing of magnetic field analysis. Analysis flow chart of iron loss solver for calculation of iron losses has two patterns

Magnetic field analysis with iron loss condition

In short it is method that executes magnetic field analysis and iron loss analysis at once. Salient steps in calculation of iron losses with magnetic field analysis having iron loss condition are as under

1. Magnetic field analysis study is done that can be also static analysis , transient response analysis and frequency response analysis using FEMM model of 3-dimensional, 2-dimensional or axis-symmetric.

2. Parameters are set for magnetic field analysis for reference for calculation of iron losses as per set procedure in [6].

3. Iron loss conditions and other necessary parameters are set as per settings illustrated in [6].

4. Finally magnetic field analysis study is executed using JMAG designer, JMAG scheduler or command line.

In this method magnetic field analysis is done first then iron losses are calculated using result file($*.jplot$). In other method, Iron loss analysis using reference to magnetic field analysis result are used for calculation of iron losses. Analysis are are performed step by step and after verifying results of magnetic field analysis, iron losses are calculated after creating study of iron losses from magnetic field analysis as per set procedure in [6].

2.7.3   Advance methods for iron loss calculation

There are formulas for both hysteresis loss and eddy current loss respectively. It is introduced and enlisted as under:

1. Hysteresis loss Formula There are four methods for hysteresis loss calculation using JMAG i.e. FFT, apply loop, hysteresis model and user subroutine.

2. Eddy current loss formula (joule loss formula). There are also four methods for joule loss calculation i.e. FFT, Maximum value,lamination analysis, and user subroutine.

3. However if iron loss table is selected for loss type in JMAG, frequency separation method is used for calculation of hysteresis and joule loss separately.

2.7.4 Hysteresis loss calculation

For iron loss calculation, firstly hysteresis loss formulas are described as under:

1. **When FFT is selected for Hysteresis loss calculation**

   It can be calculated using four approaches i.e. iron loss formula, iron loss table and hysteresis loss or joule loss table.

   (a) **Using Iron loss formula**

      Firstly calculated method is set to FFT i.e. frequency analysis and iron loss equation is chosen in loss type material editor in JMAG. The formula that is used is shown as under in eq:2.39

      $$Wh[W] = \sum_{e=1}^{nelem} \left\{ \sum_{k=1}^{N} (Kh \times |B_k|^\alpha \times f_k^\beta \times V_e) \right\} \tag{2.39}$$

      where,

      V_e is volume of each element[m^3]

      N is maximum frequency order

      Multiplier or co-efficients of of empirical formula :α and β

      nelem denotes the number of elements used.

      B_k is magnetic flux density (T) for frequency order of k:

      $$|B_k| = \sqrt{B_k * B_k^*} \tag{2.40}$$

      where,

      B_k is a complex number after FFT is performed on each component of magnetic flux density.

      B_k^* is complex conjugate of numbers of B_k

(b) **Using iron loss table**

In this method loss type is set to iron loss table in the material editor. The formula that is used in this case is as under:

$$Wh[W] = \sum_{e=1}^{nelem} \left\{ \sum_{k=1}^{N} (a(|B_k|) \times f_k \right\} \times V_e \qquad (2.41)$$

where,

$a(|B_k|$ denotes the co-efficient of magnetic flux density $|B_k|$ determined by frequency separation method.

(c) **using hysteresis loss/Joule loss(eddy current loss) table**

In this method hysteresis loss is calculated in similar manner as other FFT methods but loss type is chosen as hysteresis or joule loss table.

The formula that is used to calculate iron loss in this case is as under :

$$Wh[W] = \sum_{e=1}^{nelem} \left\{ \sum_{k=1}^{N} (Wh_e(|B_k|, f_k) \times V_e \right\} \qquad (2.42)$$

where, $Wh_e\left(B_k, \frac{1}{T}\right)$ represents the hysteresis loss density specified at the magnetic flux density B_k and frequency f_k

2. **Hysteresis loss calculation using Apply loop method**

It can also be calculated using three formulas i.e. iron loss formula, iron loss table and hysteresis loss or joule loss table.

(a) **Using iron loss formula for each magnetic flux density component**

Iron loss condition for hysteresis loss calculation method is set to 'apply loop' method and loss type is set to iron loss equation.Following Iron loss

45

formula is used when amplitudes for each magnetic flux density component are considered as shown in 2-12. Relation is as under:

$$Wh[W] = \sum_{e=1}^{nelem} \left\{ f \sum_{l=1}^{nloop} (Kh \times B_k^\alpha \times V_e) \right\} \tag{2.43}$$
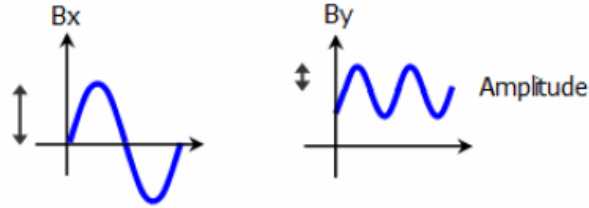
Figure 2-12: Illustration for considering amplitudes of magnetic flux density waveforms

(b) **Using iron loss formula for magnitude of magnetic flux density**

when maximum value of magnetic flux denisty is considered following formula is used in calculation of iron losses using JMAG.

$$Wh[W] = \sum_{e=1}^{nelem} \{f \times Kh \times B_{max}^\alpha \times V_e\} \tag{2.44}$$

It is further illustrated in figure:2-13 as under:
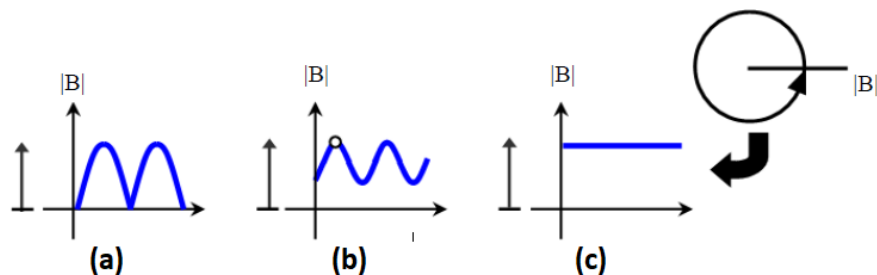
Figure 2-13: Illustration for (a) sine wave magnetic field (b) sine wave magnetic field with offset (c) Constant magnitude such as rotational magnetic field

where,

Both equation 2.43 and 2.44 the key notations description as follows:

- f is basic frequency [Hz]

- B_k is Amplitude of $K_t h$ loop (k=1-nloop) for each component of magnetic flux density.

- B_{max} is maximum value of magnetic flux density(T)

- Kh is co-efficient of hysteresis loss is equal to constant or Kh($|B_k|$,f_k)

(c) **Using iron loss table for each component of magnetic flux density**

Iron loss table is used for calculation of iron loss using each component of magnetic flux density. The relation is as under:

$$Wh[W] = \sum_{e=1}^{nelem} \{f \sum_{k=1}^{nloop} a(B_k) \times V_e\} \tag{2.45}$$

The illustration is same as depicted in figure 2-12

(d) **Using iron loss table for magnitude of magnetic flux density**

Iron loss calculation is done using magnitude of magnetic flux density using iron loss table. Its relation is mentioned as under:

$$Wh[W] = \sum_{e=1}^{nelem} \{f \times a(B_{max}) \times V_e\} \tag{2.46}$$

Its illustration is shown in figure 2-13

where,

a(B) is co-efficient of magnetic flux density B determined by frequency separation method.

(e) **Using hysteresis or joule loss table for each magnetic flux density component**

Apply loop method is set in hysteresis loss calculation method and loss type is set to hysteresis or joule loss table in FEMM tool i.e. JMAG. Hence when amplitude of magnetic flux density is intended for calculation of iron loss, following relation will be taken into account as under:

$$Wh[W] = \sum_{e=1}^{nelem} \{Wh_e(B_k, f) \times V_e\} \qquad (2.47)$$

Its illustration is clearly shown in figure: 2-12

(f) **Using hysteresis or joule loss table for magnitude of magnetic flux density**

When maximum value of magnetic flux density is assumed then following relation will be used while calculating iron losses using hysteresis or joule loss table using JMAG.

$$Wh[W] = \sum_{e=1}^{nelem} \{Wh_e(B_{max}, f) \times V_e\} \qquad (2.48)$$

its illustration is shown in figure:2-13

3. **Calculation of hysteresis losses using hysteresis model method**

Calculation of hysteresis loss is done using magnetic field analysis result involving magnetic flux density history and from hysteresis curve in material property.

2.7.5   Joule loss calculation

For iron loss calculation, Now joule loss calculation is done using methods and formulas enlisted as under

It is also calculated using four methods i.e. FFT , maximum value, lamination analysis, and user sub-routine.

1. **Joule loss calculation using FFT**

   It is based on three approaches iron loss formulas, iron loss table and joule loss table or hysteresis loss table.

   (a) **Using iron loss formula**

   Iron loss condition is set to FFT, frequency analysis and loss type to iron loss equation in JMAG tool. The iron loss formula which is used in calculation of joule loss is as under:

   $$We[W] = \sum_{e=1}^{nelem} \left\{ \sum_{k=1}^{N} \left(Ke \times |B_k|^{\gamma} \times f_k^{\delta} \times V_e \right) \right\} \qquad (2.49)$$

   (b) **Using iron loss table**

   Iron loss condition is set to Iron loss table for joule loss as calculation method and loss type in material editor is set to iron loss table in JMAG tool.

   $$We[W] = \sum_{e=1}^{nelem} \left\{ \sum_{k=1}^{N} \left(b(|B_k|, f_k) \times f_k^2 \right\} \times V_e \qquad (2.50)$$

   where,

   $b(|B_k|, f_k|)$ is determined by frequency separation method, co-efficient at frequency f_k

(c) **using hysteresis loss/Joule loss table**

Iron loss condition is set to FFT and loss type to hysteresis/joule loss table in JMAG tool's material editor. The formula for determination of loss in this case is mentioned as under:

$$We[W] = \sum_{e=1}^{nelem} \left\{ \sum_{k=1}^{N} \{We_e(B_k, f_k) \times V_e \right\}$$ (2.51)

2. **Joule loss calculation using maximum value**

It is based on maximum value of magnetic flux density considered for each component. Three types of formulas are used to calculate joule loss in this case. Formulas are as under

(a) **Using iron loss formula**

Formula for calculation of joule loss considering maximum value of magnetic flux density is as under:

$$We[W] = \sum_{e=1}^{nelem} \left\{ \sum_{k=1}^{N} (Ke \times B_{max}^{\gamma} \times f^{\delta} \times V_e) \right\}$$ (2.52)

where,

B_{max} —- maximum value of each component of magnetic flux density at the interval.

$B_{max} = \sqrt{B_1^2 + B_2^2 + B_{3max}^2}$

(b) **Using iron loss table**

similarly, respective conditions are set in JMAG tool and following iron loss table formula is considered in calculation of joule loss using maximum value.

$$We[W] = \sum_{e=1}^{nelem} [\{b(B_{max}, f) \times f^2\} \times V_e)]$$ (2.53)

50

$b(B_{max}, f)$ is determined by frequency separation method, co-efficient at frequency f

(c) **using hysteresis/joule loss table**

iron loss condition is set to maximum value for joule loss calculation method and loss type is set to hysteresis/joule loss table.

The formula used to determine loss is as follows:

$$We[W] = \sum_{e=1}^{nelem} [\{We_e(B_{max}, f) \times V_e\}] \qquad (2.54)$$

3. **Using lamination analysis**

Loss distribution of internal magnetic steel sheet is utilized for calculation of joule loss (eddy current loss). It is estimated using electric and magnetic properties along with magnetic flux density analysis result.

All methods for calculation of iron losses using iron loss solver are discussed briefly in aforementioned sections sourced from [6]. However procedure is summarized using flow chart in figure 2-14
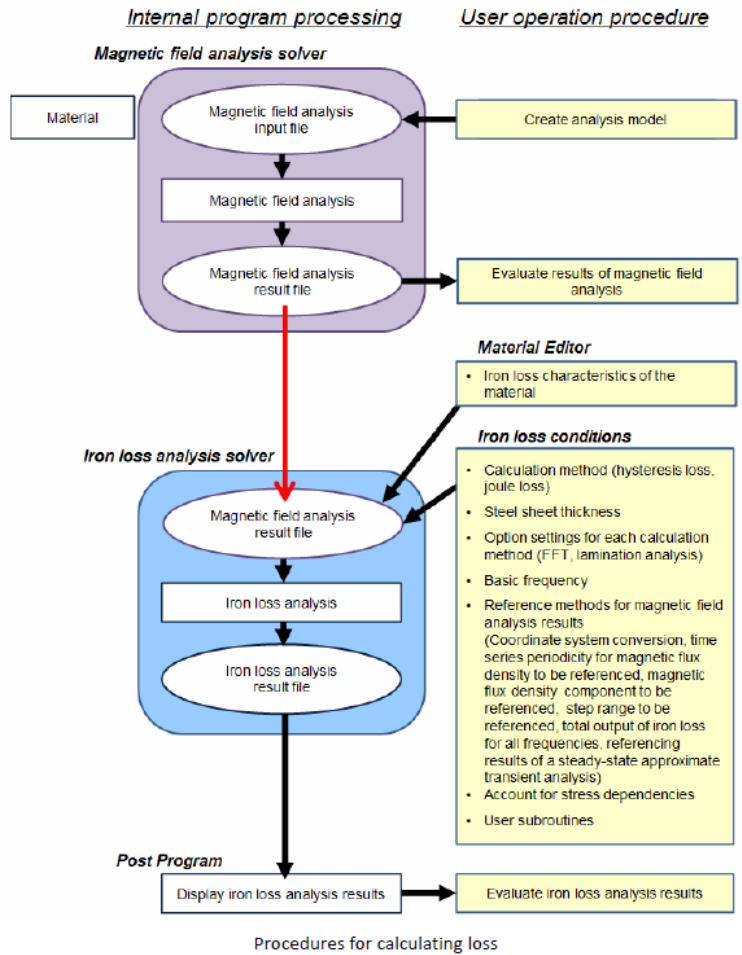
Figure 2-14: Procedure to calculate loss using iron loss solver [6]

2.8 Conclusion

All iron loss models discussed in literature are summarized according to their ability to operate with complex waveforms, prior material knowledge for calculation of losses and respective accuracies in table 2.1.

Table 2.1: Extended version of the table in [8]

Iron loss model	Complex wave-forms	Material prior knowledge	Accuracy	Section
steinmetz equation [2.5]	-	small	low	2.3
Fourier transform-steinmetz equation(FTSE) [2.5]	-	small	low	2.3.6
Modified steinmetz equation(MSE)[2.11]	+	small	low medium	2.3.1
Generalized steinmetz equation(GSE)[2.15]	-	medium	low medium	2.3.2
Improved generalized steinmetz equation (iGSE) [2.16]	+	medium	low medium	2.3.3
Natural steinmetz extension (NSE)[2.19]	+	medium	low medium	2.3.4
Improved-Improved generalized steinmetz equation(i^2GSE) [2.22]	+	high	medium	2.3.5
steinmetz premagnitization graph(SPG)[2.24]	+	high	medium	2.3.7
Loss separation model [2.30]	-	medium	medium	2.5
Loss surface model[2.4]	+	high	medium-good	2.4
Preisach model[2.35]	+	high	good	2.6.1
Jiles Atherton Model[2.38]	+	high	good	2.6.2

Chapter 3

Experimental characterization of Fe-Si Sample with dc bias

3.1   General test setup for measurement of core losses

B-H loop measurement is considered suitable method for measurement of core losses because of its simplicity and rapid measurements. Test setup includes power stage (incorporating power amplifier and controller), power supply and rectangular sheet sample in single sheet coil tester. It is depicted in figure 3-1
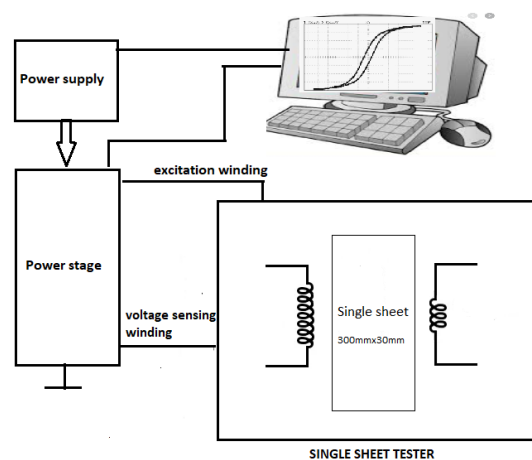
Figure 3-1: Test setup based on general principle of single sheet testing
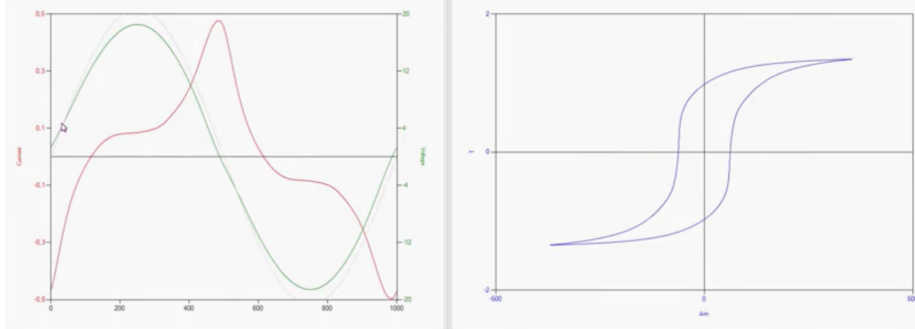
Figure 3-2: Sinusoidal measurement with digital feedback control

3.2 Test bench description

High precision test bench i.e. state of the art facility used in house to carryout material characterization.Its specification are shown in Table-3.1. Same test bench was used by authors in [7]. It is based on high bandwidth linear power amplifier which is IEC 60404 certified. is adopted for estimation of losses. Measurement of losses are done using single sheet sample for high high frequency ranges and high magnetic flux densities. MPG is expert software and test bench is a product of brockhaus manufacturer. It enable user to set up the coil system i.e single sheet tester and to enter definition of sample under test including definition of measurement sequence. In addition to it, it enables High induction sinusoidal measurement with digital feedback Control as shown in figure 3-2. Furthermore, measurement of losses can be done under different type of excitations and with free curves.

Table 3.1: Test bench features

Parameter	Capacity
Fundamental frequency	5KHz to 100KHz
Low frequency amplifier capacity	100V/52A peak
Fundamental Excitation(up to 20KHz)	60V 40A,(continuous)
High frequency amplifier capacity	50V/10A
Non-sinusoidal/PWM(up to 100KHz)	peak and continuous
Operating temperature: soft magnetic materials	-40 °C to 180 °C
Hard magnetic materials	-40 °C to 180 °C
Operating stress(compression): Soft magnetic materials	0 to 3 kN
Hard magnetic materials	0 to 1 kN
Excitation waveform capability	Sine wave, DC/Normalized PWM Harmonic injection

3.3   Properties of rectangular Single sheet sample

Rectangular single sheet sample is made up of single lamination of Fe-Si steel(manufactured in house). Measurement of specific total loss is carried out as per IEC standard 6404-3 [14]. Properties of sheet under test are depicted in Table 3.2.

Table 3.2: Properties of rectangular Sheet under test

Name	Property
Magnetic material	10JNEX900
weight	6.741g
density	7490 kg/m^3
primary winding	128
secondary windings	102
magnetic length	0.241 m
Cross section	$3mm^2$
length	300mm
width	30mm
thickness	0.1mm
Volume(V_e)	$900mm^3$
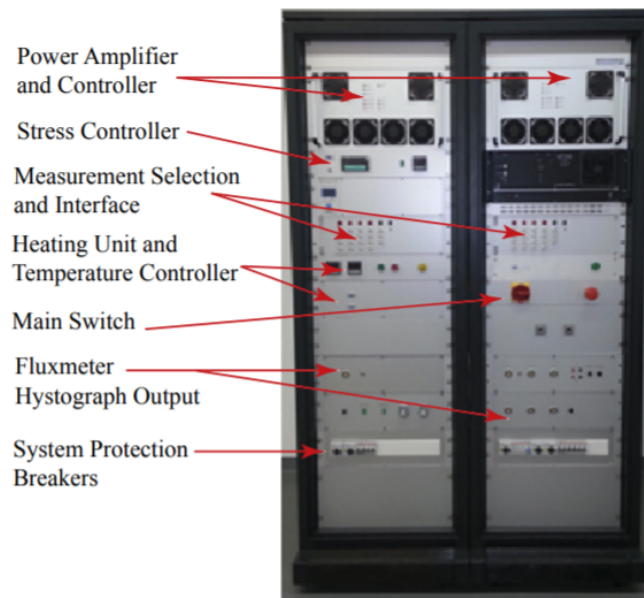
Figure 3-3: Test bench used for experimentation [7].

3.4 DC characterization

First of all, DC characterization is done to get the B-H curve from low excitation level up-to saturation point for maximum magnetic field intensity i.e. 500 A/m. As shown in figure 3-4. that saturation point is 1.212 T which is achieved at quite lower magnetic flux density of 160 A/m in data sheet of manufacturer shown in figure 2-3 but in close agreement for both data sheet and experimental DC hysteresis loop in case of lower magnetic field strengths. These variations in hysteresis loops of data sheet and experimental data are due to manufacturing effects in magnetic material.

Figure 3-4: DC Hysteresis loop of 10JNEX900

3.5   Ac characterization with dc bias

Ac characterization is done for measurement of losses at 100 Hz with dc bias of 0 A/m for flux density range of up to 1 T with 0.1 T increment. Similarly, Losses are recorded for frequency range of up to 2000 Hz using sinusoidal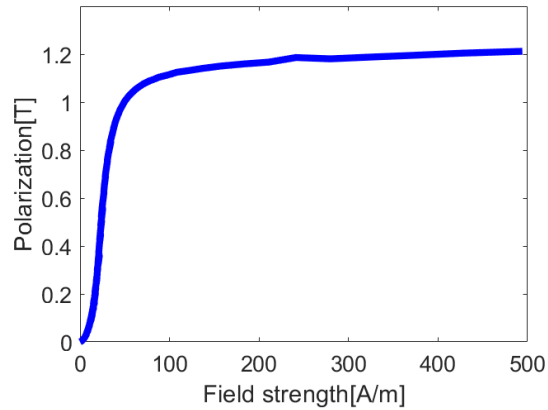 excitation waveform. Test bench will ensure good form factor. Basically primary current and secondary voltage are recorded to get B-H loop.Mainly, Losses are calculated under area of B-H loop and other losses would be eddy current losses and excess losses. Measurement of losses are done under dc bias (premagnitization) of 10 A/m, 30 A/m, 40 A/m and 50 A/m with respect to high frequency range of 100 Hz, 300 Hz, 500 Hz, 700 Hz, 1100 Hz, 1500 Hz, and 2000 Hz respectively. Total specific loss is represented as function of frequency as shown in figure 3-5a. Measured losses up to 2000 Hz for range of premagnitization H_{dc} of 0 A/m to 50 A/m are depicted in figure 3-5.

Data obtained as result of ac characterization with dc offset will be taken into account in section-3.7 for obtaining variation of steinmetz parameters as result of dc offset present in minor loops of non-sinusoidal flux densities or test signals.
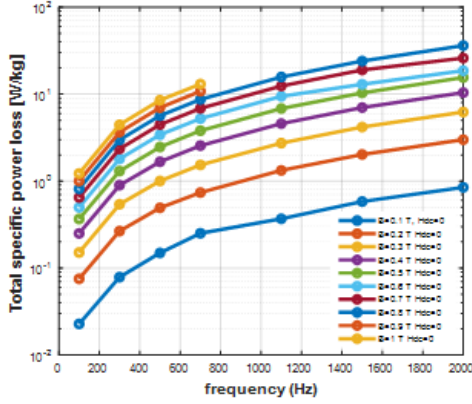
(a) For H_{dc}=0 A/m
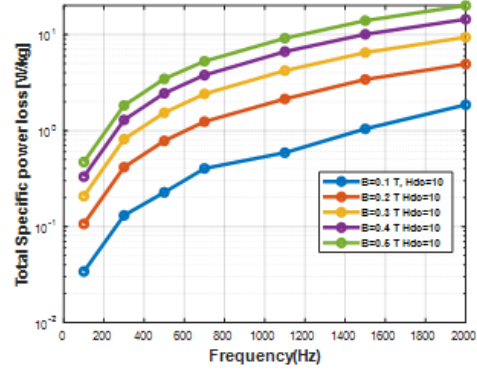
(b) For H_{dc} =10 A/m
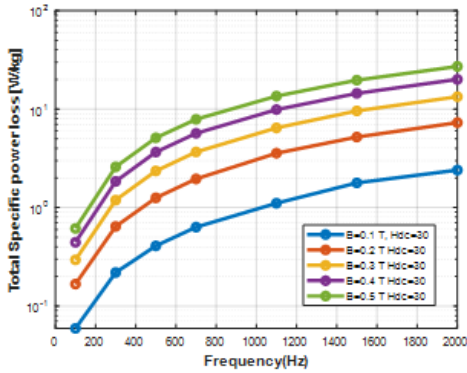
(c) For H_{dc} =30 A/m
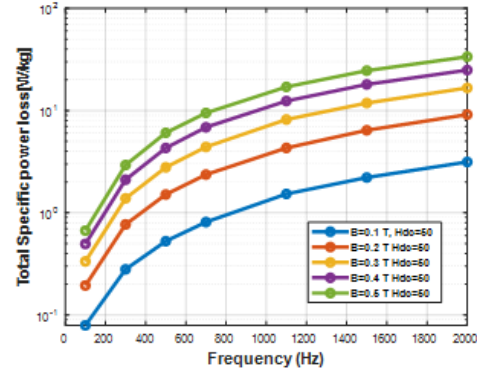
(d) For H_{dc} =50 A/m

Figure 3-5: Core loss with and without dc bias condition (measured for 10JNEX900 magnetic material (Fe-Si with 6.5% si content) using rectangular single sheet sample

3.6 Measurement of total specific power losses

Test signals are used for calculation of losses that will be used as benchmark experimental losses against loss data estimated by iGSE with dc bias condition method in chapter-4. All test signals has fundamental frequency of 100 Hz. Five different types of waveforms are used with different harmonic order.These waveforms are listed with respective harmonic components in Table-3.3 as under ;

Furthermore,B-H curves of All five waveforms are depicted in figure-3-6. It is noted that B-H curve of waveform with 100Hz,500Hz has no minor-loop and has larger area where larger losses are estimated. It is noted that major loops have no dc bias unlike minor loops.

59

Table 3.3: Total specific loss[W/kg] of Magnetic flux density waveforms(100 Hz) with harmonic orders

waveforms	Frequency components (Hz)	Total specific loss[W/kg]
01	100, 300	1.0660
02	100, 500	1.8505
03	100, 300, 500	1.2764
04	100, 300, 700	1.4486
05	100, 300, 500, 700	1.2536
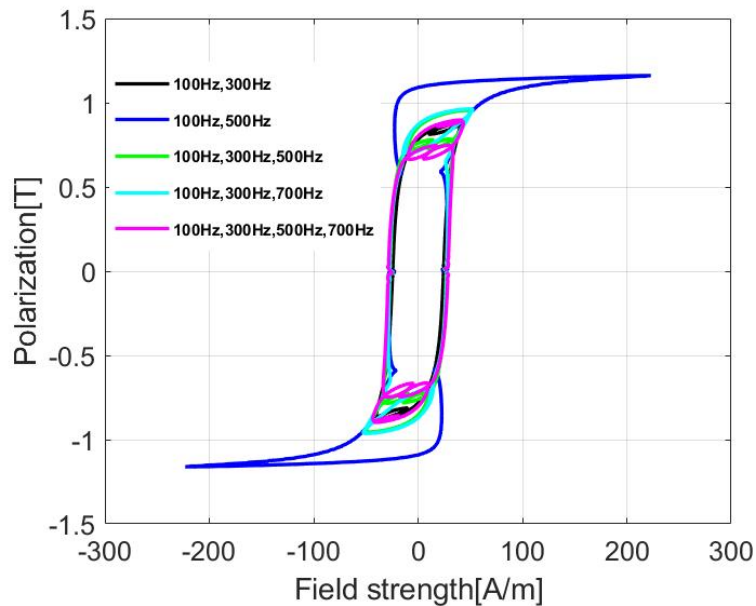
Figure 3-6: Magnetization curves of Test signals

It is further explained in chapter-4.

3.7   Determination of steinmetz parameters due to dc bias offset

The best fit steinmetz parameters vary with frequency and under dc bias condition H_{dc}. Experimental loss data for range of magnetic field strengths i.e. 0 to 50 A/m and range of frequencies (100 Hz, 300 Hz, 500 Hz, 700 Hz, 1100 Hz, 1500 Hz, 2000 Hz) respectively are curve fitted using steinmetz equation(Power law)that yield respective best fit steinmetz parameters i.e. α ,β and k. Curve fitting tool is used in MATLAB

and corresponding best parameters are obtained in three dimensions using polynomial fit as function of flux densities,frequencies and experimental loss data. Non-linear least Squares method is used with robustness set to Least Absolute residual(LAR). Goodness of fit is ensured by closely monitoring optimum values of R-square(R^2), adjusted R-square and root mean squared error(RMSE) and sum of squares due to error (SSE).R-square(R^2) was found to be close to 1 that indicates that greater proportion of variations are accounted in surface fit by the model.Curve fitting of zero pre-magnetization loss data is depicted in figure(3-7). Similarly curve fits are obtained for pre-magnetization of 10, 30 and 50 A/m.Best fit steinmetz parameters are shown in Table-3.4.
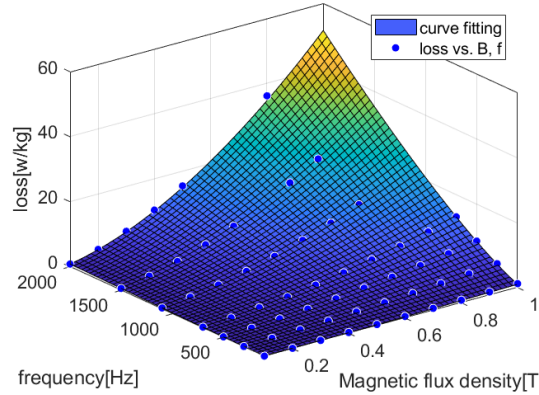
Figure 3-7: Curve fitting as function of (flux density,frequency) for experimental loss data of zero pre-magnetization (H_{dc})

Table 3.4: Best fit steinmetz parameters

Parameter	$H_{dc} = 0$ A/m	$H_{dc} = 10$ A/m	$H_{dc} = 30$ A/m	$H_{dc} = 50$ A/m
α	1.308	1.278	1.221	1.261
β	1.776	1.54	1.464	1.476
k	0.002488	0.003553	0.007189	0.006762

For zero pre-magnetization ($H_{dc} = 0A/m$), loss data for range of flux densities up to 1 T is considered whereas other ranges of premagnitization is characterized for flux densities up to 0.5 T. Variation in steinmetz parameters i.e. alpha, beta and k is considered in calculation of losses using iGSE with dc bias condition method in chapter(4). It is because of the fact that dc bias affect losses significantly as shown

in pictorial comparison of estimated losses of conventional iGSE without dc bias and iGSE with dc bias method in 4 . Losses obtained for each frequency range are curve fitted corresponding to flux densities of up to 1 T at 100Hz under dc bias of 0 A/m, 10 A/m, 30 A/m and 50 A/m respectively.Furthermore, goodness of fit statistics are obtained as shown in table(3.5). Goodness of fit for R-square method and adjusted R square method is between 0 and 1, where 1 is regarded as the best curve fitting.In addition to it, Sum of squares due to error(SSE) goodness of fit ranges are open ended where zero is regarded as the best surface fitness that would give small random error in prediction. In addition to it, 0 is regarded as the best fitness for RMSE method too. Overall fitness shows optimum statistics in our curve fitting for range of premagnization shown in table-3.5.

Table 3.5: Goodness of fit statistics for best fit steinmetz parameters

Methods(Goodness of fit)	$H_{dc} = 0$	$H_{dc} = 10$	$H_{dc} = 30$	$H_{dc} = 50$
R-square(R^2)	0.9996	0.9996	0.9999	0.9998
Sum of squares due to error(SSE)	1.284	0.2918	0.1825	0.4962
Adjusted R-square	0.9996	0.9996	0.9999	0.9998
Root mean squared error(RMSE)	0.1451	0.09549	0.07552	0.1245

3.8   Conclusion

In this chapter, experimental results are shown and steinmetz parameters due to dc bias condition are calculated. It is found from curve fitting results shown in table 3.4 that all steinmetz parameters are changing due to dc bias condition H_{dc}. Therefore, it is important to consider variation of steinmetz parameters in calculation of losses using iGSE. It is further explained in chapter 4 where iGSE with dc bias method is developed and losses are estimated and compared.

Chapter 4

Core loss prediction using iGSE under dc bias condition (iGSEDC)

4.1 Introduction

The new method is proposed to consider dc bias condition in non-sinusoidal magnetic flux density waveforms to improve the core loss prediction using iGSE.This method under dc bias condition is known as improved generalized steinmetz equation with dc bias condition (iGSEDC). It involves variation of steinmetz parameters using mean amplitude of each separated major and minor loop flux density waveform corresponding to premagnitization H_{dc} range of up to 50 A /m. Initially, premagnitization (i.e. H_{dc}) is obtained from B-H loop based polynomial curve fit equation as function of dc bias present in magnetic field density waveforms. Then steinmetz parameters(α, β, k) are obtained from each polynomial curve fit equations based on Steinmetz parameters as function of premagnitization H_{dc}. Steinmetz parameters as function of premagnitization H_{dc} are shown in table-3.4.

Variation of Steinmetz parameters as function of premagnetization H_{dc} is also shown in figure 4-1. These graphs are used to get polynomial curve fit equations of each Steinmetz parameter(α, β, k) as function of H_{dc}. It is important to note that major loop does not have dc bias. In other words, mean amplitude of major loop waveform is zero. The polynomial equations serve as to map the respective steinmetz

parameters for respective dc bias (mean amplitude) of each minor loop waveform.

(a) k as function of H_{dc}

(b) α as function of H_{dc}

(c) β as function of H_{dc}
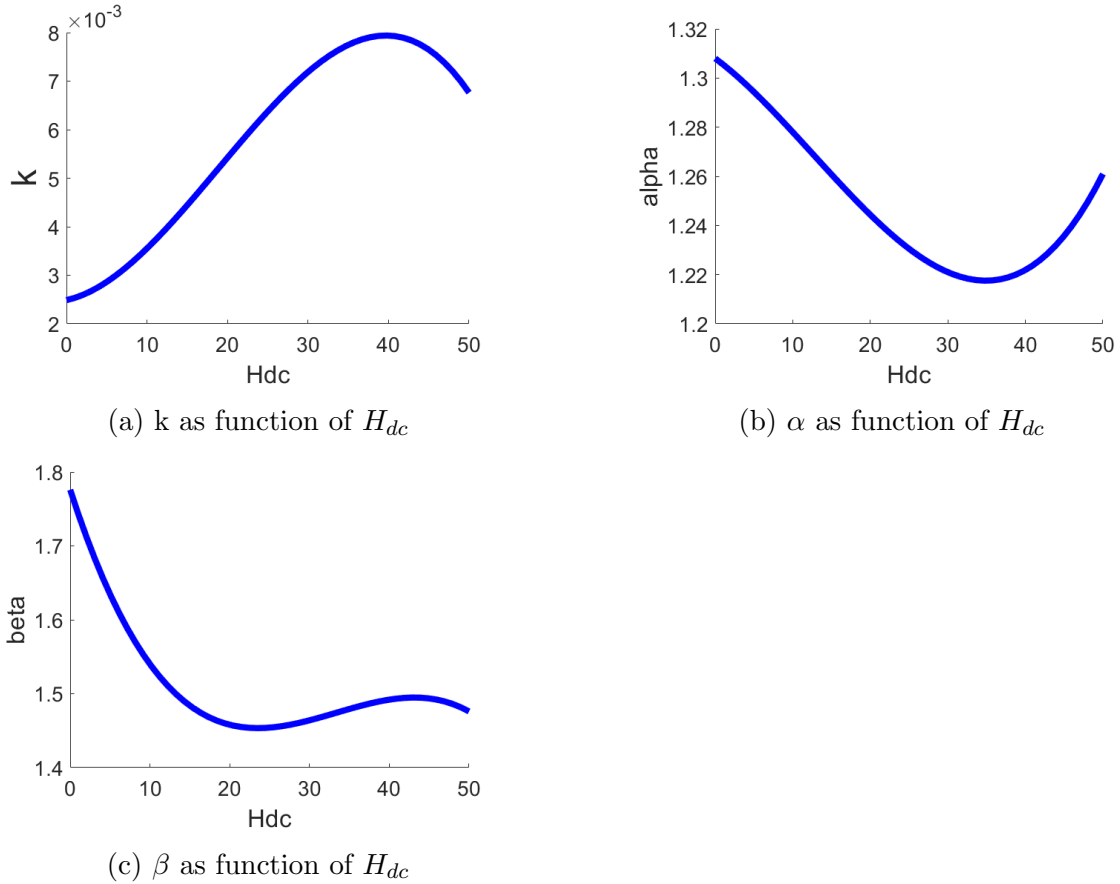
Figure 4-1: Steinmetz parameters (k, α, β) as function of premagnitization (H_{dc})

4.2 Explanation of test signals with corresponding major and minor loops

There are five test signals used for experimentation and corresponding losses were used as benchmark values compared to core loss estimation using frequency domain method i.e. Fourier transform steinmetz equation (FTSE), improved generalized steinmetz equation (iGSE) and improved generalized steinmetz equation under dc bias condition(iGSEDC). All test signals can be viewed in terms of Δ slope for ease of understanding and differentiating one test signal from other. All test signals are illustrated in following sub sections.

Test signal 01: Increasing and decreasing slopes

First test signal is the fundamental and third harmonic composite waveform.Respective quadrants are shown corresponding to B-H loop in figure 4-2. Experimental losses for this waveform are for nominal flux density of 0.871 T and magnetic field strength(A/m) of 40 A/m.

(a) 100 Hz waveform with 300 Hz component

(b) B-H loop of 100 Hz, 300 Hz
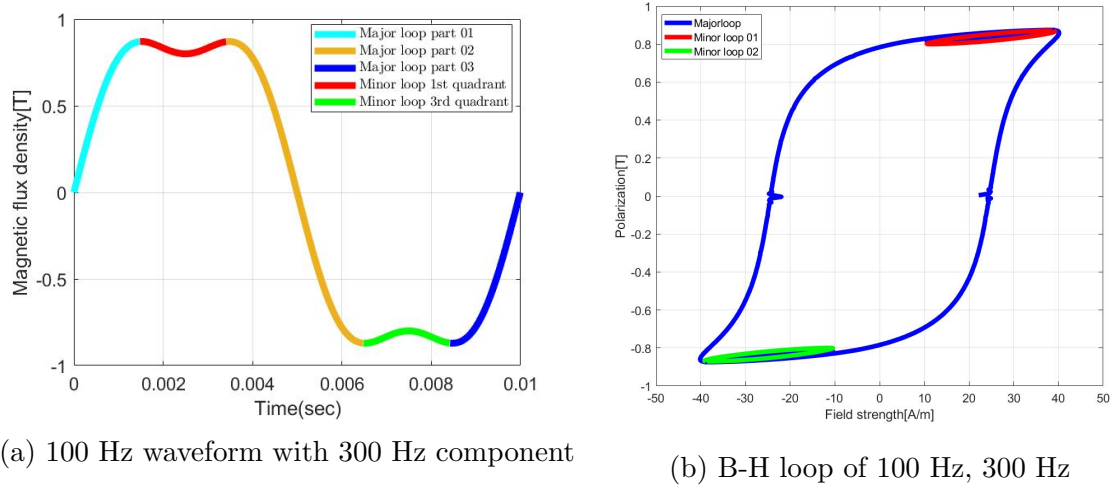
Figure 4-2: Test signal 01

Test signal 02: Increasing and increasing slopes

In this Test signal, waveform is based on fundamental frequency component of 100 Hz with fifth harmonic order.Respective quadrants are shown corresponding to B-H loop. It is vivid in figure 4-3 that the test signal has no minor loops.It is solely based on major loop but with little deviations. Experimental losses for this waveform are for nominal flux density of 1.15 T and magnetic field strength of 223.06 A/m.

It is clear that signal slopes are increasing and increasing again. In this signal, harmonic distortion due to fifth harmonic amplitude is 14.95 %.

(a) 100 Hz waveform with 500 Hz component

(b) B-H loop of 100 Hz, 500 Hz
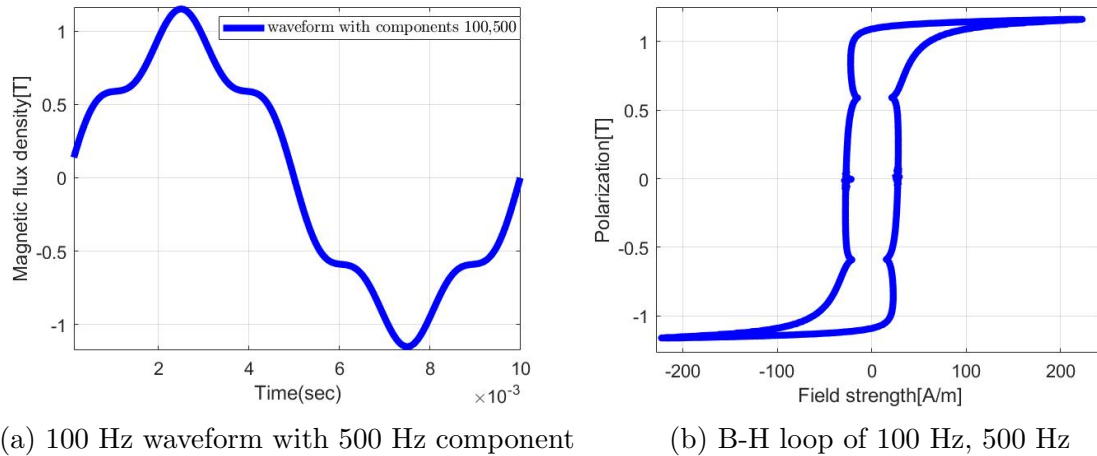
Figure 4-3: Test signal 02

Test signal 03: Increasing , decreasing and increasing slopes

This composite waveform is based on fundamental component of 100 Hz with harmonic components of 300 Hz and 500 Hz. Test signal with major loop and minor loops is illustrated pictorially as under ;

(a) 100 Hz waveform with 300 Hz and 500 Hz component

(b) B-H loop of 100 Hz, 300 Hz, 500 Hz components

Figure 4-4: Test signal 03

It is observed that slope of this waveform is increasing,decreasing and increasing again in sequential manner. All changes in slope are defined with respect to 1st quadrant. Experimental loss is obtained for this non-sinusoidal waveform with nominal
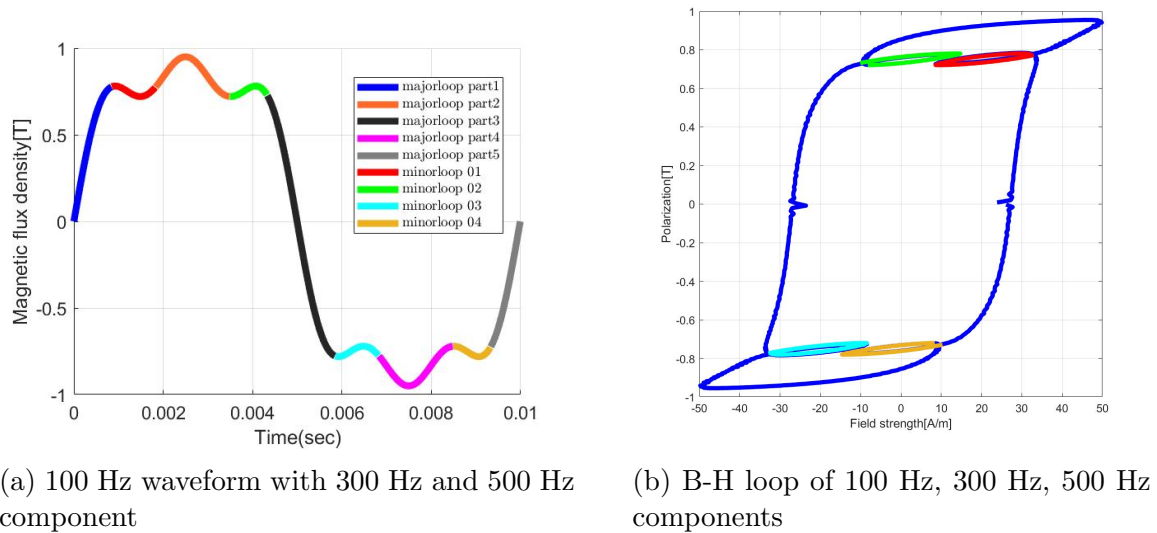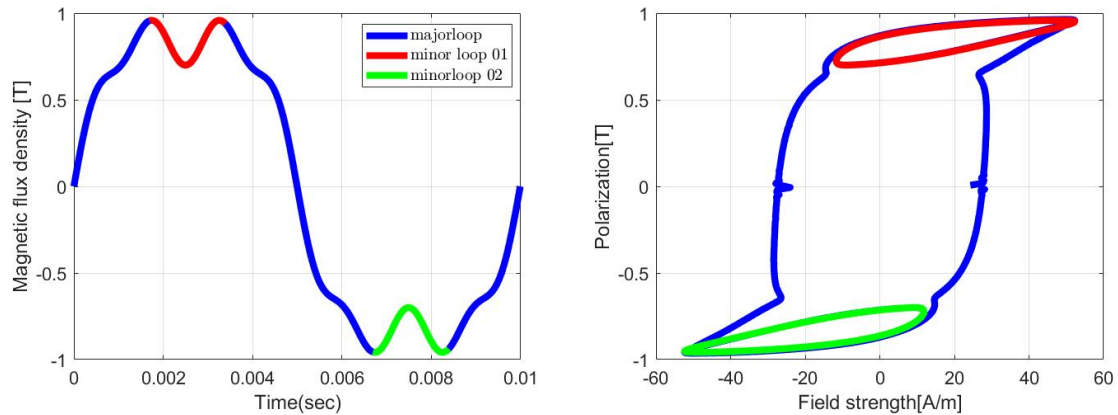
flux density of 0.95 T and magnetic field strength (A/m) of 49.8 A/m.

Test signal 04: Increasing,increasing and decreasing slopes

This test signal is based on fundamental component of 100 Hz with harmonic components of 300 Hz & 700 Hz. Signal with major loop and minor loops are illustrated pictorially as under:

(a) 100 Hz waveform with 300 Hz and 700 Hz component

(b) B-H loop of 100 Hz, 300 Hz, 700 Hz components

Figure 4-5: Test signal 04

Hence, this signal has two slope changes in 1st quadrant. First it increases then it decreases.Experimental loss is determined for this particular waveform under nominal flux density of 0.96 T and magnetic field strength(A/m) of 52.3 A/m.

Test signal 05: Increasing, decreasing ,increasing and decreasing slopes

It is based on composite waveform of fundamental component of 100Hz with harmonic components of 300 Hz, 500 Hz and 700 Hz. Signal with major loop and minor loops is illustrated pictorially as under ;

Clearly slope changes are four i.e. increasing, decreasing, increasing and decreasing slopes. All in 1st quadrant. These slope changes marks the start of respective minor loops in 1st quadrant.Experimental losses for this waveform are for nominal flux density of 0.89 T and magnetic field strength (A/m) of 43.3 A/m.
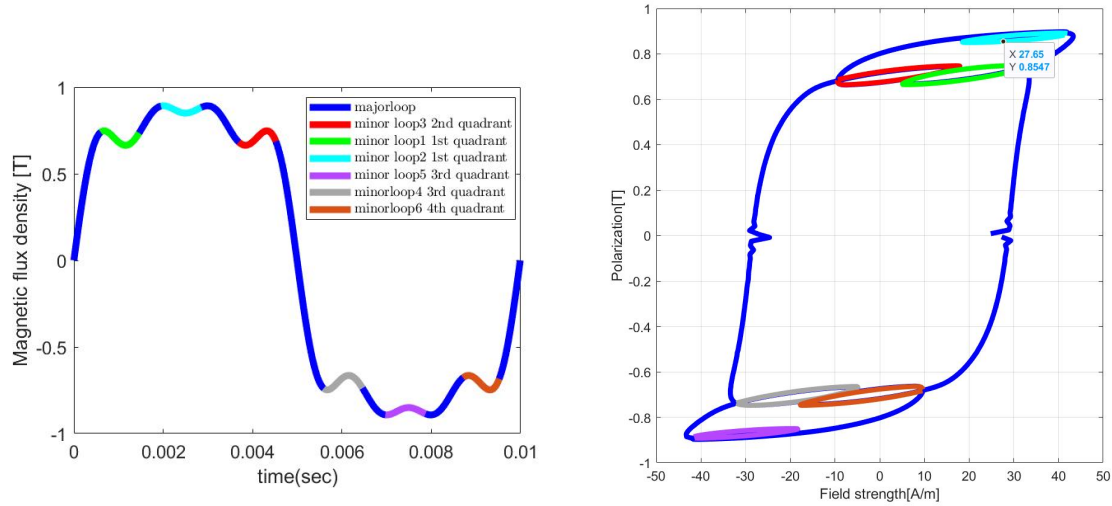
(a) 100 Hz waveform with 300 Hz and 700 Hz component

(b) B-H loop of all components

Figure 4-6: Test signal 05

4.3   Steps to separate major and minor loops

Separation of major and minor loops are done considering 1st and 2nd quadrant flux density waveforms using change in slope first. It is done in similar fashion for 3rd and 4th quadrant but with opposite slopes. Flow chart of separation of major and minor loop is shown in figure 4-8a. In this regard, major loop and minor loops are separated with steps enlisted as under ;

1. Firstly, Magnetic flux densities corresponding to 1st quadrant and 2nd quadrant are processed for waveform depicted in figure-4-7 and respective major and minor loops are depicted in figure(4-4a).

2. When 1st quadrant of waveform in considered, first slope change is detected. If it is decreasing then it will be regarded minor loop detection. Hence, 1st maximum value is saved for extraction of 1st minor loop until waveform rise back to same flux density. Similarly more minor loops are checked using decreasing slope for 1st quadrant of waveform.

3. Similarly, if slope change is positive in 1st quadrant of waveform and flux density is rising then flux density values are regarded as major loop points and saved
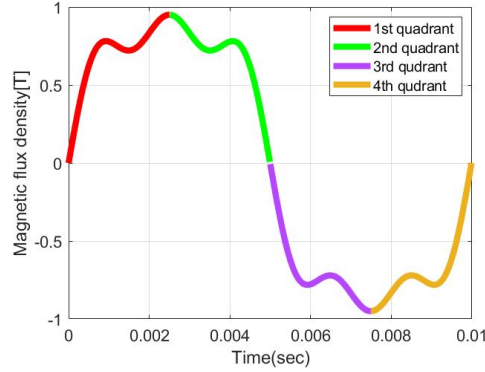
68

Figure 4-7: 100Hz waveform with 300 Hz and 500 Hz components showing all quadrants

in major loop vector.

4. When 2nd quadrant of waveform is considered. It is the case of falling waveform where first slope change is positive (increasing slope) then it is regarded as minor loop detection right in valley.Then its minor loop points are extracted starting from valley until it rise back to same flux density value.

5. Similarly major loop points for negative slopes (decreasing slope) are extracted from 2nd quadrant and saved in major loop vector as collection of all major loop points.

6. Again 3rd and 4th quadrant minor loops are obtained but with opposite slopes with respect to slope detection of 1st and 2nd quadrant. It can also be obtained from absolute values of 1st and 2nd minor loops. It is noted that all test signals depicts symmetry. Similarly, major loop points are found and extracted from 3rd and 4th quadrant. It is similar to minor loop extraction from 1st and 2nd quadrant but with opposite slopes. Separated major loop is shown in figure 4-8b.

7. Finally improved general Steinmetz equation (iGSE) with dc bias is used to calculate losses for each major and minor loop points with respective variation of best fit steinmetz parameters (k,β,α).

69
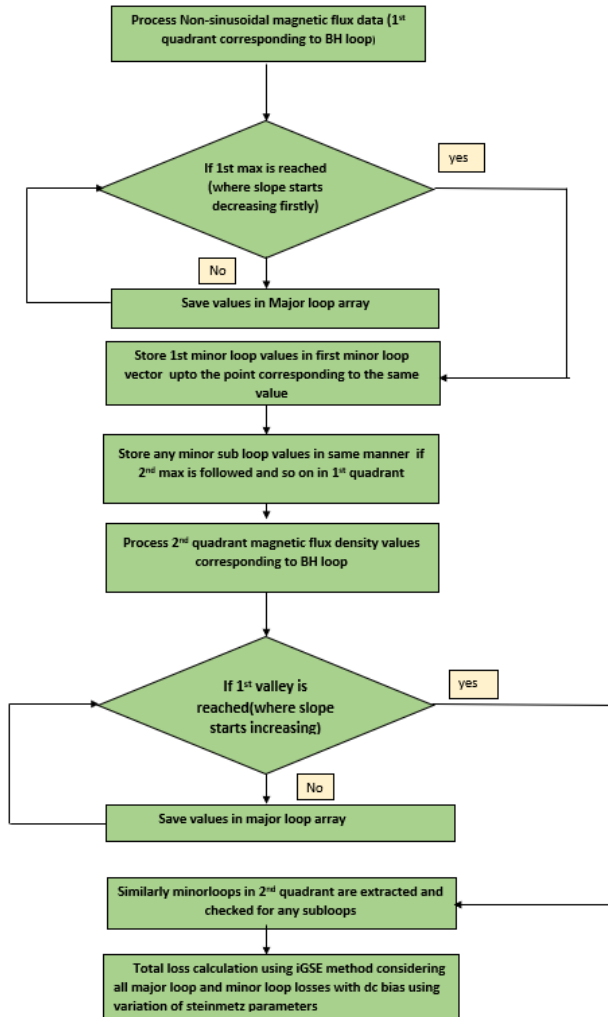
(a) Flow chart of separation of major and minor loop
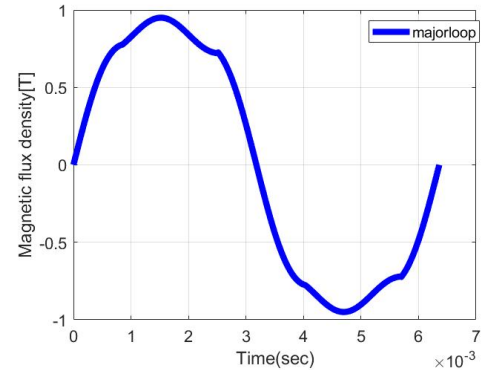
(b) Separated major loop

Figure 4-8: Steps for separation of major and minor loop (a) Flow chart for half cycle of flux density (b) Separated major loop

4.4 Equations of iGSEDC with variation of steinmetz parameters

When non-sinusoidal magnetic flux densities are separated into major and minor loops resulting in two conditions.First is that the major loop is without dc bias condition. On the other hand, minor loops are with dc bias condition. Therefore it is important

for time domain iron core loss model i.e. iGSEDC to calculate losses with and without dc bias conditions. It calculates ΔB for each major and minor loop. It yields final expression for time average loss with variation of steinmetz parameters due to dc bias condition as shown in equation 4.1. Therefore equation can be re-written for ease of understanding as under:

$$P_v(i) = \frac{1}{T(i)} \times \int_0^T k_i(i) \times \left| \frac{dB(i)}{dt(i)} \right|^{\alpha(j)} \times |\triangle B(i))|^{\beta(j)-\alpha(j)} dt(i) \qquad (4.1)$$

where,

$$k_i(i) = \frac{k(j)}{(2\pi)^{\alpha(j)-1} \int_0^{2\pi} |cos\theta|^{\alpha(j)} |2|^{\beta(j)-\alpha(j)} d\theta} \qquad (4.2)$$

Where,$\triangle$B is peak to peak magnetic flux density of major and minor loops.similarly dB/dt is calculated for each major and minor loops.ki is also obtained for each major and minor loops using equation 4.2. In equation 4.1, "i" denotes iteration size of each major and minor loop and "j" denotes the variation of Steinmetz parameters with respect to dc bias condition of each minor loop.

Total loss is found by weighted average, taking into account the contribution of major loop loss and each minor loop loss. It is calculated by using the fraction of total period each loop occupies using equation(4.3).

$$P_{total} = \sum_{n=\iota} P_\iota(i) \frac{T_\iota(i)}{T} \qquad (4.3)$$

There is no dc bias condition in major loop but DC bias condition is vivid in minor loops in test signals where mean amplitude of minor loop flux densities is not zero. It is depicted in section-4.2. It is also clear that this method is independent of superposition principle. As it calculate losses for each separated loop using equation 4.1 and then total loss is found by summing the weighted average of time period each loop occupies.

4.5 Comparison of iron loss estimation results of iGSEDC method with conventional iGSE and FTSE method

Iron loss calculations are done for conventional iGSE method, iGSEDC i.e. improved generalized steinmetz equation under dc bias condition and FTSE (Fourier transform steinmetz equation) using MATLAB script. Frequency domain core loss estimation method is compared to show importance of time domain core loss estimation. Core loss prediction of each method are compared pictorially and shown in figure 4-9.
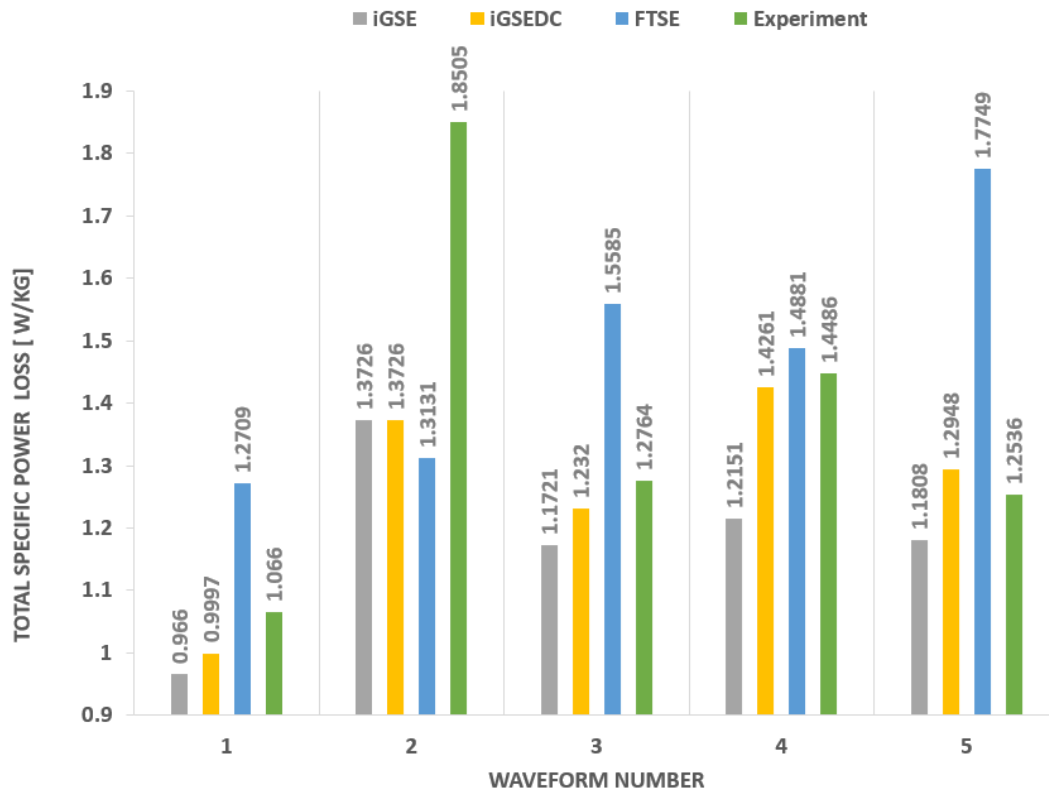

Figure 4-9: Comparison of core losses using iGSEDC, iGSE, FTSE and experiment

4.6 Comparative analysis of iGSEDC with iGSE and FTSE in terms of percentage errors

Iron loss estimation error of each iron loss model determines the accuracy of each method.It is done by using relation in equation (4.4).

$$Absolute \ \% \ error = \frac{|L_{Experiment} - L_{model}|}{L_{experiment}} \qquad (4.4)$$

Where $L_{Experiment}$ shows the losses obtained by experiments and L_{model} represents losses estimated by iron loss models.

Absolute percentage Errors are calculated using absolute difference between benchmark experimental data and core loss estimation using iGSE,iGSE under DC bias condition (iGSEDC) and FTSE model respectively. It is shown in table 4.1.

Table 4.1: Absolute percentage (%) estimation errors of iGSE, iGSEDC and FTSE with respect to experimental data

Waveform	Frequency components in Test signals	iGSEDC	iGSE	FTSE
1	100Hz,300Hz	6.2 %	9.40 %	19.2 %
2	100Hz,500Hz	25.83 %	25.83 %	29 %
3	100Hz,300Hz,500Hz	3.47 %	8.17 %	22.1 %
4	100Hz,300Hz,700Hz	1.550 %	16.12 %	2 %
5	100Hz.300Hz,500Hz,700Hz	3.29 %	5.81 %	41.6 %

In figure 4-10, Comparison is done in terms of absolute percentage(%) errors for each method namely iGSE, IGSEDC and FTSE.

IGSE under dc bias condition (iGSEDC) yield optimum results for all waveforms except the case of 2nd test signal where there are no minor loops and have considerable major loop deviations i.e. briefed in section-4.2. It is noted that iGSEDC estimate losses similar to conventional iGSE. It happens when dc biased minor loops are not present in waveform.
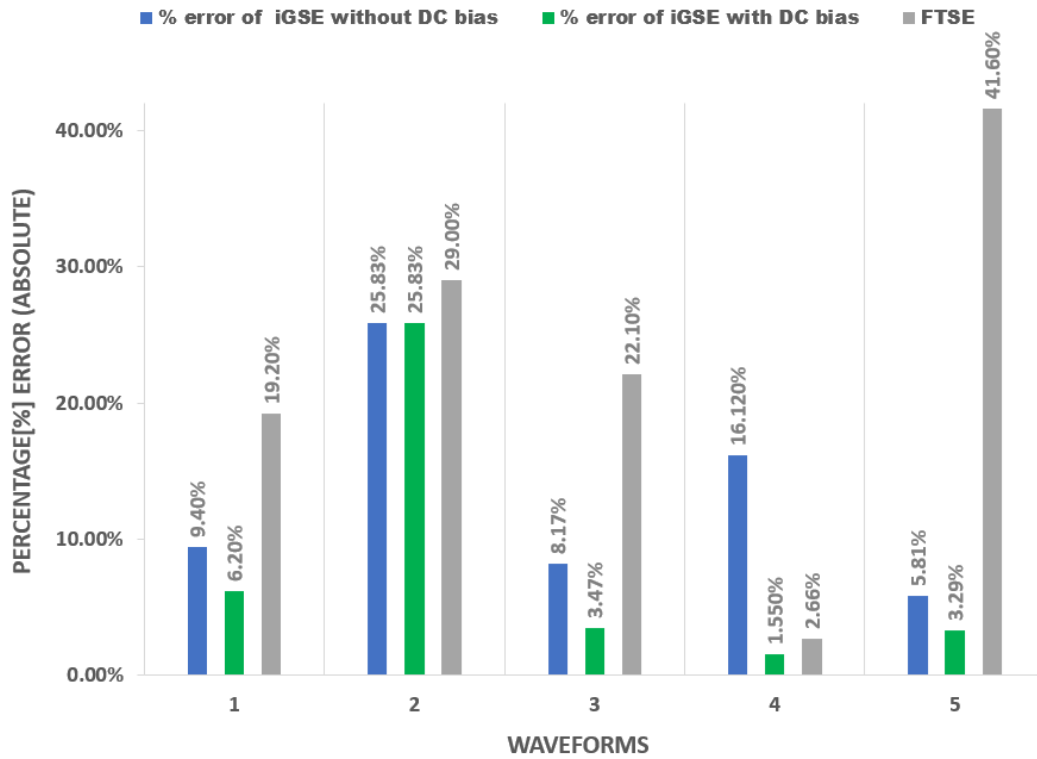
Figure 4-10: Comparison of iGSEDC, iGSE and FTSE method in terms of percentage error

4.7 Conclusion

In this chapter, It is proved that conventional iGSE method is inaccurate compared to iGSEDC.In addition to it, conventional iGSE method underestimate losses because it lacks dc bias consideration. On the other hand, FTSE is the most inaccurate method compared to iGSE and iGSEDC. It has variable trend in estimation of losses and therefore its usage is not recommended for non-sinusoidal excitation waveforms. However, It is popularly used in industries due to its simple approach. Therefore, it is recommended to calculate losses with dc bias condition using iGSEDC method. The iGSEDC method gives promising results compared to conventional iGSE and frequency domain method i.e. FTSE.

It is verified that iGSEDC don't follow superposition principle as it is based on separation of minor loops. It calculates losses due to each loop using weighted average of time period each loop occupies. This makes iGSEDC method calculates losses near

knee point of the B-H curve well below saturation region which corresponds to real operation of the electrical machine.On the other hand, frequency domain method i.e. FTSE calculate losses due to fundamental loop and harmonic loop causing calculation of losses around origin of B-H loop that is in disagreement of real operation of machine. Therefore frequency domain method should not be followed. It is illustrated as below;
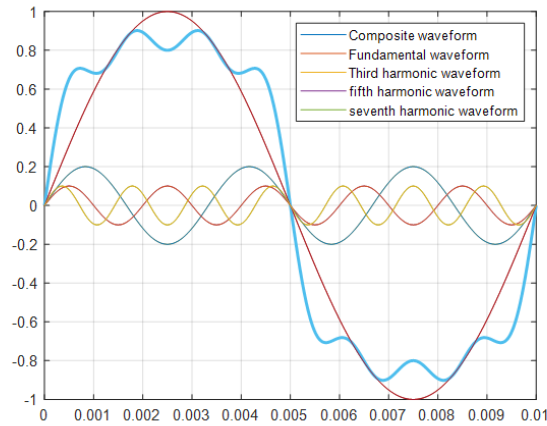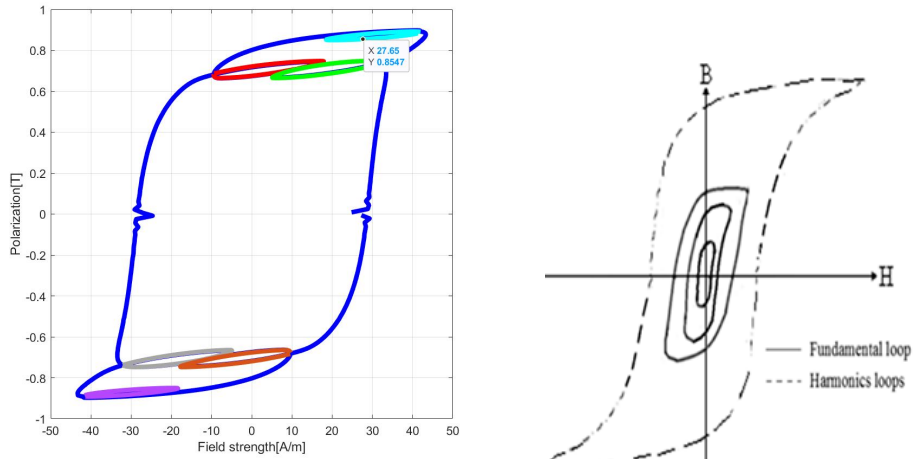

Figure 4-11: Harmonic waveforms & composite waveform

(a) BH loop due to composite waveform with minor loops

(b) BH loop due to individual harmonic waveforms

Figure 4-12: Comparison between BH loop based on harmonic waveforms and composite waveform

Chapter 5

Future Outlook

5.1 Design of interior permanent magnet machine

Prediction of core losses using iGSE with dc bias can be extended for calculation of iron losses in motors by extracting the flux densities from any designed motor. The existing Case study of JMAG motor model[33] i.e. IPM motor is used. During design process of IPM motor, 6.5% silicon content based Fe-Si magnetic alloy is used i.e. 10JNEX900 as stator core and rotor core material. Interior permanent magnet motor specifications are shown in Table(5.2) are shown. In addition to it, all the material properties are set from material properties table 5.2. Designed motor is shown in figure(5-1b).

Table 5.1: Specification of IPM motor

Number of poles	4
Number of stator slots	24
Connection pattern	Y-Connection
Phase resistance of the coil	0.814 Ohm
Number of the turns	35
Power supply	4A ,three phase Ac excitation
Rotation speed	1800 r/min
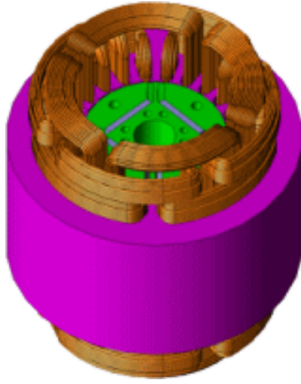
(a) Model of interior permanent magnet (IPM) motor
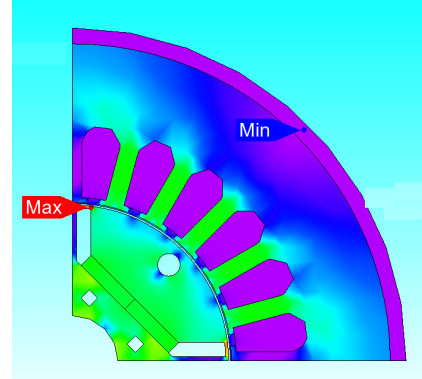
(b) 2D Interior permanent magnet motor for analysis

Figure 5-1: Design of Interior permanent magnet motor

Table 5.2: Material properties of each part in designed IPM motor

Part	Magnetic property	others
Rotor core	JNEX steel(10JNEX900)	lamination factor laminated core:98%
stator core	JNEX steel(10JNEX900)	lamination factor laminated 98%
Magnet	$JSOL : NdFeB_B r = 1.4(T)$	Orientation: Parallel Pattern (Circular Direction)
Coil	Copper	-

5.2 Extraction of magnetic flux density waveform from tooth of stator

After the design process of IPM motor, active study is executed. respective rated conditions such as power and torque is checked and working of motor is verified. Using Probe, magnetic flux density is extracted for element ID of 2924 i.e. tooth of the stator. That is where the magnetic flux density is maximum and is regarded as saturated region (green) as indicated in figure(5-1b). Similarly B-H loop with respective minor loops can be seen using B-H probe for hysteresis loss calculation.
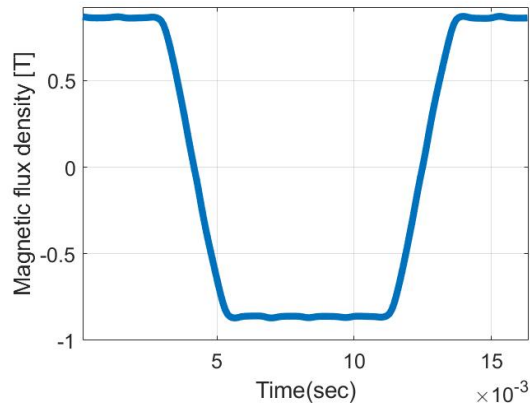
Figure 5-2: Extracted magnetic flux density from teeth of IPM motor

5.3   Conclusion

Fast fourier transform is performed on extracted magnetic flux density. In this regard, respective frequency components and amplitudes are found as shown in figure 5-3. Therefore significant frequency components and respective amplitudes can be used to reconstruct harmonic flux density waveform and processed into algorithm of iGSEDC method for loss estimation in stator tooth of motor.Similarly it can be done for several rotor positions with FEMM simulations for getting flux waveforms in stator and rotor core with respective variation for one electrical cycle.Experiments can be performed using extracted flux waveforms using test bench and then iGSEDC method can be used for calculating losses of IPM motor for respective extracted test signals.
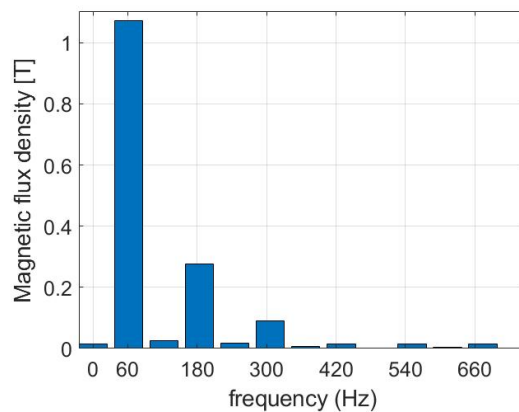

Figure 5-3: Amplitude spectrum of extracted flux density of stator tooth

Chapter 6

Conclusion

iGSEDC (Improved generalized Steinmetz equation under DC bias condition) is also named as hybrid iron loss method. It is suited for non-sinusoidal flux density waveforms in electrical machines where major loop don't have dc bias condition unlike minor loops. It is concluded that variation of steinmetz parameters (α, β, k) should be taken into account in calculation of losses to take into account the dc bias condition. It is present in minor loops of non-sinusoidal excitation waveforms of electrical machines. Results involves all non-sinusoidal excitation waveforms having fundamental frequency of 100 Hz.

Compared to experiment, estimation results show that iGSE under dc bias condition (iGSEDC) err by 6.2 % unlike 9.4 % error of conventional iGSE method and 19.2 % error of FTSE for test signal with third harmonic order. Similarly, In case of test signal with fifth harmonic order, iGSEDC and conventional iGSE performs and estimate losses similarly as there are no minor loops. Therefore, both iGSE and iGSEDC yield errors of 25.8 % unlike 29 % error of FTSE. It is observed in loss estimation of test signal with third and fifth harmonic order that iGSEDC estimate losses with an error of 3.47 % unlike iGSE and FTSE where estimation errors are 8.17 and 22.1 % respectively. In case of test signal where third and seventh harmonic orders are involved, loss estimation errors of iGSEDC,iGSE and FTSE are 1.55 %, 16.12 % and 2 % respectively.Furthermore, the test signal where third,fifth,seventh harmonic orders are present, iGSEDC performs better than iGSE and FTSE with estimation errors

of 3.29 %, 5.81 % and 41.60 % respectively. Hence, it is concluded that iGSE under dc bias condition (iGSEDC) turns out to be the most accurate method compared to conventional iGSE and FTSE.

Future works of iGSEDC can be extended for experiments and core loss estimation under different types of non-sinusoidal excitation waveforms. One crucial form of waveform excitation is Pulse Width Modulation (PWM) for power electronics converters.

Bibliography

[1] JFE.Steel-Corporation, *Magnetic Property Curves Super Core Grades*, 2020 (accessed 17 July, 2020). [Online]. Available: https://www.jfe-steel.co.jp/en/products/electrical/catalog/f2e-001.pdf

[2] JFE-Steel-Corporation, *Electrical Steel Sheets for high frequency Application*, 2020 (accessed 17 July, 2020). [Online]. Available: https://www.jfe-steel.co.jp/en/products/electrical/catalog/f1e-002.pdf

[3] A. Krings and J. Soulard, "Overview and comparison of iron loss models for electrical machines," *Journal of Electrical Engineering*, vol. 10, pp. 162–169, 05 2010.

[4] K. Venkatachalam, C. R. Sullivan, T. Abdallah, and H. Tacca, "Accurate prediction of ferrite core loss with nonsinusoidal waveforms using only steinmetz parameters," in *2002 IEEE Workshop on Computers in Power Electronics, 2002. Proceedings.*, 2002, pp. 36–41.

[5] F. Krall, "Analysis and implementation of algorithms for calculation of iron losses for fractional horsepower electric motors," Master's thesis, Graz University of Technology, 2017.

[6] JSOL-corporation, *JMAG version 18.0 user's Manual of iron loss formulas (accessed from installation folder).* JMAG division,JSOL Corporation, 2019.

[7] N. Fernando, G. Vakil, P. Arumugam, E. Amankwah, C. Gerada, and S. Bozhko, "Impact of soft magnetic material on design of high-speed permanent-magnet machines," *IEEE Transactions on Industrial Electronics*, vol. 64, no. 3, pp. 2415–2423, 2017.

[8] A. Krings, "Iron losses in electrical machines— influence of material properties,manufacturing processes,and inverter operation," Ph.D. dissertation, KTH Royal Institute of Technology, 2014.

[9] EVI-IEA, *Paris electromobility declaration*, 2020 (accessed September, 2020). [Online]. Available: https://iea.blob.core.windows.net/assets/f46a8513-4d12-4a64-8402-92f4672695dc/paris-electro-mobility-declaration.pdf

[10] A. Boglietti, A. Cavagnino, and A. Krings, "New magnetic materials for electrical machines and power converters," *IEEE Transactions on Industrial Electronics*, vol. 64, no. 3, pp. 2402–2404, 2017.

[11] A. Krings, A. Boglietti, A. Cavagnino, and S. Sprague, "Soft magnetic material status and trends in electric machines," *IEEE Transactions on Industrial Electronics*, vol. 64, no. 3, pp. 2405–2414, 2017.

[12] A. Krings, M. Cossale, A. Tenconi, J. Soulard, A. Cavagnino, and A. Boglietti, "Magnetic materials used in electrical machines: A comparison and selection guide for early machine design," *IEEE Industry Applications Magazine*, vol. 23, no. 6, pp. 21–28, 2017.

[13] N. Fernando and F. Hanin, "Magnetic materials for electrical machine design and future research directions: A review," in *2017 IEEE International Electric Machines and Drives Conference (IEMDC)*, 2017, pp. 1–6.

[14] IEC-6404-3, *Magnetic materials-Part 3: Methods of measurement of the magnetic properties of magnetic sheet and strip by means of a single sheet tester*, 3rd ed. International Electrotechnical Commission(IEC), 2018.

[15] C. P. Steinmetz, "On the law of hysteresis," *Proceedings of the IEEE*, vol. 72, no. 2, pp. 197–221, 1984.

[16] J. Reinert, A. Brockmeyer, and R. W. A. A. De Doncker, "Calculation of losses in ferro- and ferrimagnetic materials based on the modified steinmetz equation," *IEEE Transactions on Industry Applications*, vol. 37, no. 4, pp. 1055–1061, 2001.

[17] Jieli Li, T. Abdallah, and C. R. Sullivan, "Improved calculation of core loss with nonsinusoidal waveforms," in *Conference Record of the 2001 IEEE Industry Applications Conference. 36th IAS Annual Meeting (Cat. No.01CH37248)*, vol. 4, 2001, pp. 2203–2210 vol.4.

[18] M. Mu and F. C. Lee, "A new core loss model for rectangular ac voltages," in *2014 IEEE Energy Conversion Congress and Exposition (ECCE)*, 2014, pp. 5214–5220.

[19] M. Smailes, C. Ng, R. Fox, J. Shek, M. Abusara, G. Theotokatos, and P. Mckeever, "Evaluation of core loss calculation methods for highly nonsinusoidal inputs," in *11th IET International Conference on AC and DC Power Transmission*, 2015, pp. 1–7.

[20] S. Yue, Y. Li, Q. Yang, X. Yu, and C. Zhang, "Comparative analysis of core loss calculation methods for magnetic materials under nonsinusoidal excitations," *IEEE Transactions on Magnetics*, vol. 54, no. 11, pp. 1–5, 2018.

[21] J. Muhlethaler, J. Biela, J. W. Kolar, and A. Ecklebe, "Improved core-loss calculation for magnetic components employed in power electronic systems," *IEEE Transactions on Power Electronics*, vol. 27, no. 2, pp. 964–973, 2012.

[22] A. Van den Bossche, V. C. Valchev, and G. B. Georgiev, "Measurement and loss model of ferrites with non-sinusoidal waveforms," in *2004 IEEE 35th Annual Power Electronics Specialists Conference (IEEE Cat. No.04CH37551)*, vol. 6, 2004, pp. 4814–4818 Vol.6.

[23] J. Muhlethaler, J. Biela, J. W. Kolar, and A. Ecklebe, "Core losses under the dc bias condition based on steinmetz parameters," *IEEE Transactions on Power Electronics*, vol. 27, no. 2, pp. 953–963, 2012.

[24] T. chevalier, A. kedous-lebouc, B. cornut, and C. Cester, "A new dynamic hysteresis model for electrical steel sheet," *Physica B: Condensed Matter*, vol. 275, no. 1, p. 197–201, 2000.

[25] G. Bramerdorfer and D. Andessner, "Accurate and easy-to-obtain iron loss model for electric machine design," *IEEE Transactions on Industrial Electronics*, vol. 64, no. 3, pp. 2530–2537, 2017.

[26] H. Jordan, "Die ferromagnetischen konstanten für schwache wechselfelder," *Elektrische Nachrichtentechnik*, vol. 1, p. 8, 1924.

[27] G. Bertotti, "General properties of power losses in soft ferromagnetic materials," *IEEE Transactions on Magnetics*, vol. 24, no. 1, pp. 621–630, 1988.

[28] L. Petrescu, V. Ionita, E. Cazacu, and C. Petrescu, "Steinmetz' parameters fitting procedure for the power losses estimation in soft magnetic materials," in *2017 International Conference on Optimization of Electrical and Electronic Equipment (OPTIM) 2017 Intl Aegean Conference on Electrical Machines and Power Electronics (ACEMP)*, 2017, pp. 208–213.

[29] I. D. Mayergoyz, *Mathematical Models of Hysteresis and Their Applications*. Elsevier, 2003.

[30] D. C. Jiles and J. B. Thoelke, "Theory of ferromagnetic hysteresis: determination of model parameters from experimental hysteresis loops," *IEEE Transactions on Magnetics*, vol. 25, no. 5, pp. 3928–3930, 1989.

[31] F. R. Fulginei, G. M. Lozito, S. Gaiotto, and A. Salvini, "Improving the jiles-atherton model by introducing a full dynamic dependence of parameters," in *2015 IEEE 1st International Forum on Research and Technologies for Society and Industry Leveraging a better tomorrow (RTSI)*, 2015, pp. 161–165.

[32] G. Torrisi, S. Mariéthoz, and R. Smith, "Identification of magnetic characteristics of induction motors based on the jiles-atherton model," in *2014 16th European Conference on Power Electronics and Applications*, 2014, pp. 1–10.

[33] JMAG-international, *PM motor 2D analysis- Self learning case study*, 2020 (accessed august, 2020). [Online]. Available: https://www2.jmag-international. com/support/sls/v191/documents_en/source/2dmotor/op.html